Field Crops Research 234 (2019) 73–86

Contents lists available at ScienceDirect

Field Crops Research

journal homepage: www.elsevier.com/locate/fcr

Newly developed water productivity and harvest index models for maize in an arid region

Hui Ran[a], Shaozhong Kang[b,*], Xiaotao Hu[a,*], Fusheng Li[c], Taisheng Du[b], Ling Tong[b], Sien Li[b], Risheng Ding[b], Zhenjiang Zhou[d], David Parsons[e]

[a] Key Laboratory of Agricultural Soil and Water Engineering in Arid and Semiarid Areas, Ministry of Education, Northwest A&F University, Yangling, 712100, China
[b] Center for Agricultural Water Research in China, China Agricultural University, Beijing, 100083, China
[c] College of Agriculture, Guangxi University, Nanning, Guangxi, 530005, China
[d] College of Biosystems Engineering & Food Science, Zhejiang University, Hangzhou, 310058, China
[e] Department of Agricultural Research for Northern Sweden, Swedish University of Agricultural Sciences, SE-901 83, Umeå, Sweden

ARTICLE INFO

Keywords:
AquaCrop
Harvest index model
Water productivity model
Water stress
Yield simulation

ABSTRACT

Simulating yield response to different irrigation scenarios is important for agricultural production, especially in the arid region where agriculture depends heavily on irrigation. To better predict yield under different irrigation scenarios, the variation of normalized water productivity (WP^*) over the whole growing period of maize for seed production and the effect of different irrigation treatments on harvest index (HI) were investigated using field experiments from 2012 to 2015 in an arid region of northwest China. Two new non-linear dynamic WP^* ($WP^*_{KR\text{-}L}$ and $WP^*_{KR\text{-}S}$) models derived from the Logistic and Sigmoid equations, and four new HI ($HI_{KR\text{-}J}$, $HI_{KR\text{-}M}$, $HI_{KR\text{-}B}$ and $HI_{KR\text{-}S}$) models developed on the basis of water deficit multiplicative or additive models at different growth stages were compared with the measurements and the WP^* (WP^*_{AC}) and HI sub-model (HI_{AC}) in the original AquaCrop model (Version 4.0). In addition, the WP^*_{AC} and HI_{AC} models in the original AquaCrop model were replaced by the optimal WP^* and HI models to build the AquaCrop-KR model. Then the yield simulated by the AquaCrop-KR model was compared with the measured yield and the yield simulated by the original AquaCrop model. The results show that both $WP^*_{KR\text{-}L}$ and $WP^*_{KR\text{-}S}$ models improved the simulation of final biomass, especially for the $WP^*_{KR\text{-}L}$ model. The tested HI sub-models, namely $HI_{KR\text{-}J}$, $HI_{KR\text{-}M}$, $HI_{KR\text{-}B}$ and $HI_{KR\text{-}S}$ models had good performance to simulate HI under different irrigation scenarios, and the $HI_{KR\text{-}M}$ model was the best among all tested sub-models. When both $WP^*_{KR\text{-}L}$ and $HI_{KR\text{-}M}$ sub-models were embedded into Aquacrop, the performance of the AquaCrop model was improved significantly to simulate yield, especially under severe water stress condition, with R^2 increased from 0.496 to 0.653, NRMSE decreased from 26.2% to 16.1% and EF increased from 0.055 to 0.642.

1. Introduction

Water resources are scarce in arid areas where agriculture heavily relies on irrigation (Kang et al., 2017; Ran et al., 2017a) and water has always been the key factor limiting crop production in much of the world where precipitation is insufficient to meet the needs of crops (Steduto et al., 2012). High-precision crop models can be used to optimize irrigation schedules and manage crop production in those regions. With the development of crop transpiration simulation models, water-driven crop models which capture the basic features of the response of crops to water can be useful. The AquaCrop model developed by FAO (Steduto et al., 2009; Raes et al., 2009), is currently a widely used water-driven crop model, and is well balanced between simplicity (less parameters needed) and accuracy (Hsiao et al., 2009; Araya et al., 2010; Andarzian et al., 2011; Abedinpour et al., 2012; Wang et al., 2013; Mabhaudhi et al., 2014; Tavakoli et al., 2015; Toumi et al., 2016). However, calibration is still needed before applying the model, especially under severe water stress conditions (Heng et al., 2009; Katerji et al., 2013).

In the AquaCrop model, the accumulated biomass has a linear relationship with normalized crop transpiration (T/ET_0), with the slope defined as the normalized water productivity (WP^*), which is considered to be constant across the life of the crop, for specific crop species (Steduto et al., 2009). However, Hsiao et al. (2009) found a variation in WP^* during the growing period of maize, with an increasing WP^* at the start, followed by a constant WP^* and declined WP^* close to

* Corresponding authors.
E-mail addresses: kangsz@cau.edu.cn (S. Kang), huxiaotao11@nwsuaf.edu.cn (X. Hu).

https://doi.org/10.1016/j.fcr.2019.02.009
Received 29 June 2018; Received in revised form 8 February 2019; Accepted 10 February 2019
Available online 19 February 2019
0378-4290/

maturity. Katerji et al. (2013) showed that the AquaCrop model can better simulate the maize biomass accumulation well during the first half of the growth period, but significantly over-estimates the biomass accumulation during the latter half of the growth period. This is in agreement with our previous study on maize for seed production, implying a decreased accuracy of biomass simulation, if WP^* is set to be a fixed parameter over the whole growing period (Ran et al., 2018). Considering the variation of WP^* during the crop growing period might be an alternative way for better simulation of biomass.

Harvest index (HI), which is defined as the ratio of yield to final biomass, is widely used for yield forecasting in crop models. HI is affected by crop variety, and abiotic stresses. (DeLougherty and Crookston, 1979; Muchow, 1989; Bolaños and Edmeades, 1993; Kang et al., 2000; Farré and Faci, 2006; Ran et al., 2016). Although a number of models can estimate HI (Richards and Townley-Smith, 1987; Sadras and Connor, 1991; Kemanian et al., 2007), simulating HI is still a challenge under water-stressed conditions. In the AquaCrop model, HI under water stress is calculated by modifying the reference HI (HI_0) by the water stress coefficient calculated from soil water content (Raes et al., 2009). Some studies have suggested that an adjustment of HI_0 is required when using AquaCrop for yield simulation under water-stressed conditions (Hsiao et al., 2009; Farahani et al., 2009; Araya et al., 2010). Our previous study also found that the HI simulated by AquaCrop is nearly unchanged regardless of the degree of water stress, which substantially reduces the accuracy of yield simulation especially for water stress treatments (Ran et al., 2018). Therefore, it is necessary to develop a HI model that better capture the effects of water stress at different stages on HI.

Thus, the variation of WP^* over the whole growing period of maize for seed production and the effect of different irrigation treatments on HI were investigated to improve the simulation accuracy of yield in regions of water shortage. The objectives of this study were to (1) develop new non-linear dynamic WP^* models derived using Logistic and Sigmoid equations ($WP^*_{KR\text{-}L}$ and $WP^*_{KR\text{-}S}$), and new HI models based on water stress multiplicative ($HI_{KR\text{-}J}$ and $HI_{KR\text{-}M}$) or additive ($HI_{KR\text{-}B}$ and $HI_{KR\text{-}S}$) models at different growth stages. These new WP^* and HI models were compared with the original AquaCrop WP^* (WP^*_{AC}) and HI sub-model (HI_{AC}) respectively based on the measured biomass and HI, and (2) build AquaCrop-KR based using the newly developed WP^* and HI models, and compare it with the original AquaCrop on the performance of yield simulation.

2. Description of WP^* and HI models

2.1. Normalized water productivity (WP^*) model

The relationship between crop biomass and normalized transpiration (T/ET_0) is established based on the data in a large field equipped with an eddy covariance (EC) system (Exp. 1) each year from 2012 to 2015 (the details of Exp. 1 is described in Section 3.1.), using the method recommended by Hsiao et al. (2009) (Fig. 1). Considering the soil evaporation is marginal as a result of over 70% of the surface covered by a film-mulch in the experimental field (Jiang et al., 2016a; Ran et al., 2017b), crop transpiration (T) in Fig. 1 adopts EC measured evapotranspiration for parameterization. Statistical analysis shows that using "S" curves to fit the data are significant better than linear model for most years (Table 1). We hypothesize that the relationship between accumulated biomass and standardized transpiration is in line with the "S" curve, correspondingly, WP^* is assumed to vary along the growth stages. In this study, two WP^* models are tested: Logistic and Sigmoid WP^* sub-models.

2.1.1. $WP^*_{KR\text{-}L}$ model

The Logistic equation (Thornley, 1976) is applied to the relationship between crop biomass and transpiration as follows:

$$B_t = \frac{B_0 B_m}{B_0 + (B_m - B_0)e^{-\delta T^*}} \tag{1}$$

where B_t is the biomass accumulation (g m^{-2}), B_m is the potential final biomass without water stress (g m^{-2}), B_0 is the initial biomass (g m^{-2}), δ is the potential biomass growth index, T^* is the cumulative normalized crop transpiration $\Sigma(T/ET_0)$, T is the daily crop transpiration (mm d^{-1}), and ET_0 is the calculated daily reference evapotranspiration using the FAO Penman-Monteith method (mm d^{-1}) (Allen et al., 1998).

The non-linear dynamic WP^* based on the Logistic equation, named the $WP^*_{KR\text{-}L}$ model, can be derived by taking the derivative of B_t with respect to T^*:

$$WP^*_{KR-L} = \frac{dB_t}{dT^*} = \frac{B_m B_0 \delta (B_m - B_0)e^{-\delta T^*}}{[B_0 + (B_m - B_0)e^{-\delta T^*}]^2} \tag{2}$$

2.1.2. $WP^*_{KR\text{-}S}$ model

The Sigmoid equation (Thornley, 1976) is applied to the relationship between crop biomass and transpiration as follows:

$$B_t = B_m \frac{(T^*/T_c)^\eta}{1 + (T^*/T_c)^\eta} \tag{3}$$

where T_c is the T^* value corresponding to the half-maximum response of biomass, and η is a constant.

The non-linear dynamic WP^* model based on the Sigmoid equation, named the $WP^*_{KR\text{-}S}$ model, can be derived by taking the derivative of B_t with respect to T^*:

$$WP^*_{KR-S} = \frac{dB_t}{dT^*} = \frac{\eta B_m T_c^\eta T^{*\eta-1}}{(T_c^\eta + T^{*\eta})^2} \tag{4}$$

The mathematical derivation process of $WP^*_{KR\text{-}L}$ and $WP^*_{KR\text{-}S}$ from Logistic and Sigmoid equation can be found in Appendix A.

2.1.3. WP^* in the AquaCrop model

In the AquaCrop model, WP^* is treated as a constant for maize across the whole crop growth period (Raes et al., 2012).

2.2. Harvest index model

2.2.1. $HI_{KR\text{-}J}$, $HI_{KR\text{-}M}$, $HI_{KR\text{-}B}$, and $HI_{KR\text{-}S}$ models

Quantitative relationships between harvest index and crop transpiration has been reported in literature, and it is found that, biomass partitioning to grain is physiologically coupled with water transpired (Richards and Townley-Smith, 1987; Sadras and Connor, 1991). However, these studies only consider the fraction of water transpired after anthesis. HI is found to be affected by water stress during whole growth period, and responds differently to water stress in each specific growth stage (Andersen et al., 2002; Raes et al., 2009). Pearson's product-moment correlation test shows that relative HI is significantly correlated to relative transpiration in the vegetative growth stage, flowering stage and reproductive growth stage, respectively, in this study (Table 2).

Therefore, another hypothesis of this study is drawn as (1) the quantitative relationship between HI and water stress can be expressed through crop transpiration of different stages of the whole growth period, (2) its form follows crop water production functions, and (3) sensitivity index (or coefficient) follows the pattern in FAO 33. Four new HI models are proposed based on two multiplicative-type (Jensen (1968) and Minhas et al. (1974)) and two additive-type crop water production functions (Blank (1975) and Stewart et al. (1977)). It is usually considered that soil evaporation has no direct contribution to yield formation (Perry et al., 2009; Balwinder et al., 2011; Steduto et al., 2012). Therefore, crop evapotranspiration in Jensen (1968); Minhas et al. (1974); Blank (1975) and Stewart et al. (1977) is replaced by transpiration to develop the four new HI models named $HI_{KR\text{-}J}$, $HI_{KR\text{-}M}$, $HI_{KR\text{-}B}$, and $HI_{KR\text{-}S}$ as follows:

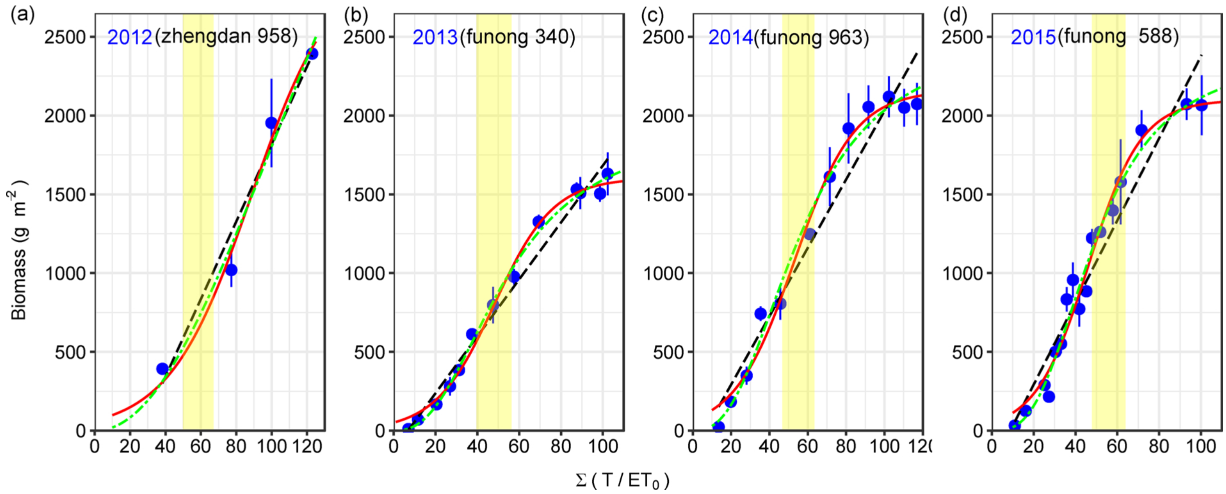

Fig. 1. Regression between measured aboveground biomass and cumulative ratio of crop transpiration (T) to reference evapotranspiration (ET_0) during biomass measurement ($\Sigma(T/ET_0)$) in a large field equipped with an eddy covariance (EC) system (Exp. 1) from 2012 to 2015. The blue points, red solid line, green dot dash line and black dashed line are measured values with error bars, fitted Logistic equation, fitted Sigmoid equation and fitted Linear equation, respectively. The light yellow band represents the flowering period. The T adopts EC measured evapotranspiration given transpiration is very close to evapotranspiration as a result of over 70% of the surface covered by a film-mulch. The varieties of 2012, 2013, 2014 and 2015 are Zhengdan 958, Funong 340, Funong 963 and Funong 588, respectively. (For interpretation of the references to colour in this figure legend, the reader is referred to the web version of this article).

$$HI_{KR-J} = \prod_{i=1}^{n} \left(\frac{T_a}{T_m}\right)_i^{\zeta_i} HI_m \tag{5}$$

$$HI_{KR-M} = \prod_{i=1}^{n} \left(1 - \left(1 - \left(\frac{T_a}{T_m}\right)_i\right)^2\right)^{\mu_i} HI_m \tag{6}$$

$$HI_{KR-B} = \sum_{i=1}^{n} \varepsilon_i \left(\frac{T_a}{T_m}\right)^i HI_m \tag{7}$$

$$HI_{KR-S} = \left(1 - \sum_{i=1}^{n} \omega_i \left(1 - \left(\frac{T_a}{T_m}\right)_i\right)\right) HI_m \tag{8}$$

where T_a is the actual crop transpiration (mm). T_m is the potential crop transpiration without water stress (mm). HI_m is the potential harvest index without water stress (%), which is a variety specific parameter. ζ_i and μ_i are the sensitivity index to water stress at each growth stage in multiplicative-type HI_{KR-J} and HI_{KR-M} models, respectively. ε_i and ω_i are the sensitivity coefficients to water stress at each growth stage in additive-type HI_{KR-B} and HI_{KR-S} models, respectively. The magnitude of ζ_i, μ_i, ε_i and ω_i for a specific growth stage would depend primarily on the sensitivity of HI to water stress during that stage. i is the ith growth stage. In this study, the whole growth period of maize is divided into vegetative growth stage, flowering stage and reproductive growth stage, which are referred to stage 1, stage 2 and stage 3, respectively.

2.2.2. HI sub-model in AquaCrop model

In the AquaCrop model, HI is calculated by modifying the reference HI (HI_0) through the water stress coefficient based on soil water content. The formula is expressed as:

Table 1
Statistical analysis of simulated and measured biomass accumulation through the regression with Logistic, Sigmoid and Linear equations from the first group of experiments (Exp. 1) during 2012 to 2015.

Year	Models	Biomass process							Final biomass	
		n	R^2	NRMSE (%)	EF	R^2_{adj}	AIC	F-Wald	n	D (%)
2012	Logistic	4	0.987	6.3	0.987	-inf	42	0.79 ($F_{0.05}(2, 1) = 199.5$, $F_{0.01}(2, 1) = 4999.5$)		
	Sigmoid	4	0.977	8.2	0.977	-inf	44	0.25 (199.5, 4999.5)		
	Linear	4	0.966	10.1	0.966	0.948	42	–		
2013	Logistic	13	0.993	6.0	0.993	0.991	108	11.20 ($F_{0.05}(2, 10) = 4.10$, $F_{0.01}(2, 10) = 7.56$)		
	Sigmoid	13	0.995	4.9	0.995	0.994	103	19.06 (4.10, 7.56)		
	Linear	13	0.977	10.8	0.977	0.975	119	–		
2014	Logistic	12	0.987	7.1	0.987	0.982	114	13.23 ($F_{0.05}(2, 9) = 4.26$, $F_{0.01}(2, 9) = 8.02$)		
	Sigmoid	12	0.986	7.4	0.986	0.980	115	11.92 (4.26, 8.02)		
	Linear	12	0.947	14.1	0.947	0.942	126	–		
2015	Logistic	17	0.976	10.3	0.976	0.970	163	12.13 ($F_{0.05}(2, 14) = 3.74$, $F_{0.01}(2, 14) = 6.51$)		
	Sigmoid	17	0.979	9.6	0.979	0.974	160	15.14 (3.74, 6.51)		
	Linear	17	0.933	17.0	0.933	0.929	176	–		
Whole	Logistic	46	0.911	20.3	0.910	0.904	499	1.63 ($F_{0.05}(2, 43) = 3.23$, $F_{0.01}(2, 43) = 5.18$)	4	−2.7
	Sigmoid	46	0.914	20.0	0.912	0.907	498	2.34 (3.23, 5.18)	4	−6.9
	Linear	46	0.903	21.0	0.903	0.901	499	–	4	8.4
Whole-standardized	Logistic	46	0.960	13.2	0.960	0.957	−239	11.18 ($F_{0.05}(2, 43) = 3.23$, $F_{0.01}(2, 43) = 5.18$)	4	−2.3
	Sigmoid	46	0.956	14.0	0.955	0.953	−234	7.54 (3.23, 5.18)	4	−6.5
	Linear	46	0.939	16.3	0.939	0.938	−224	–	4	8.9

n is number of samples, R^2 is determination coefficient, NRMSE is normalized root mean square error, EF is Nash-Sutcliffe model efficiency coefficient, R^2_{adj} is adjusted R^2, AIC is Akaike information criterion, and F-Wald is the value of Wald-Test. Values in brackets of F-Wald are F-distribution threshold at $\alpha = 0.05$ and $\alpha = 0.01$, respectively. D is the relative error. "-inf" means minus infinity. "–"means no need for calculation.

Table 2
Pearson's product-moment correlation test between harvest index (HI) and transpiration (T) of each growth stage on maize for seed production in Wuwei, Northwest China.

	Statistical test	Variables			
		$(T_a/T_m)_1$	$(T_a/T_m)_2$	$(T_a/T_m)_3$	T_a/T_m
HI_a/HI_m	r	0.52 (0.14, 0.77)	0.80 (0.57, 0.91)	0.60 (0.25, 0.81)	0.74 (0.48, 0.88)
	t	2.80 (2.08)	6.00 (2.08)	3.45 (2.08)	5.11 (2.08)
	p-value df = 21	0.011	5.8×10^{-6}	0.002	4.6×10^{-5}

HI_a is actual HI (%). HI_m is potential HI without water stress (%). T_a is the actual crop transpiration (mm), and T_m is potential crop transpiration without water stress (mm). Subscript 1, 2 and 3 represent vegetative growth stage, flowering stage and reproductive growth stage, respectively. r is the correlation coefficient, and the values inside the brackets mean 95 percent confidence interval. t is the value of student' t-test, and the value inside the brackets is the threshold of $t_{0.025\ /\ 21}$. df is degree of freedom.

$$HI = f_{HI} HI_0 \tag{9}$$

where f_{HI} is the modifying factor of the reference harvest index. Its value is determined by the time and severity of water stress (Raes et al., 2012).

2.3. Aquacrop-KR model

In the tested Aquacrop-KR model, yield is simulated as the function of crop transpiration (T), normalized water productivity (WP^*) and harvest index (HI):

$$Y = \{WP^*_{KR-L}, WP^*_{KR-S}, WP^*_{AC}\}_{opt} \times \{HI_{KR-J}, HI_{KR-M}, HI_{KR-B}, HI_{KR-S}, HI_{AC}\}_{opt} \times \sum \frac{T}{ET_0} \tag{10}$$

where $\{WP^*_{KR-L}, WP^*_{KR-S}, WP^*_{AC}\}_{opt}$ is the optimal WP^* of three tested models, $\{HI_{KR-J}, HI_{KR-M}, HI_{KR-B}, HI_{KR-S}, HI_{AC}\}_{opt}$ is the optimal five HI models, T is the crop transpiration modelled by AquaCrop, and ET_0 is the reference crop evapotranspiration.

3. Materials and methods

3.1. Experimental description

Field experiments were carried out at Shiyanghe Experimental Station of China Agricultural University, located in Wuwei city, Gansu Province, Northwest China (37°52′ N, 102°50′ E, 1581 m elevation) from 2012 to 2015. The experimental site has a typical arid inland climate and the soil texture is light sandy loam. More details about the experimental station were described in Ran et al. (2018).

Two experiments were carried out from 2012 to 2015. The aim of the first experiment (Exp. 1) was to optimize the growth stage-specific WP^* model of the AquaCrop model under full irrigation. The experiment was carried out in a large film-mulching field (300 × 300 m^2) equipped with an eddy covariance (EC) system, which was used to measure ET at daily scale. A detailed description of the EC system is provided by Ding et al. (2010), Li et al. (2013), Jiang et al. (2016b) and Ran et al. (2017b). Aboveground biomass was measured every 10 to 20 days.

The aim of the second experiment (Exp. 2) was to test the newly developed models and the original models for the prediction of biomass, harvest index and yield under different irrigation treatments. Irrigation treatments and maize cultivars varied during the period of 2012–2015. In 2012, the experiment consisted of six irrigation treatments, i.e. full irrigation (CK), deficit irrigation only at the seedling stage (SD), deficit irrigation only at the jointing stage (JD), deficit irrigation only at the heading stage (HD), deficit irrigation only at the filling stage (FD), and deficit irrigation only at the maturing stage (MD). CK was fully irrigated with 100% crop evapotranspiration (ET) during the whole growth stage. The other treatments were irrigated with 55% ET in the corresponding water stress stage as designed, and were fully irrigated as CK during the remaining stages. Maize for seed production (*Zea mays* L. cv. Zhengdan 958) was sown on April 19 and harvested on September 20, 2012. In 2013, the experiment consisted of three irrigation treatments: W1, W2 and W3. In W1, irrigation was applied up to field capacity (FC) when soil water content reached 65–70% FC; in W2, irrigation was applied up to FC when soil water content reached 55–60% FC; in W3, irrigation was applied up to FC when soil water content reached 45–50% FC. Maize for seed production (*Zea mays* L. cv. Funong 340) was sown on April 20 and harvested on September 11, 2013. In 2014, the experiment in 2013 was repeated. In addition to this experiment, a second experiment was conducted, which had four irrigation treatments, i.e. full irrigation (CK), irrigated three times at the vegetative stage (IV3), irrigated two times at the vegetative stage (IV2) and irrigated two times at the reproductive stage (IR2). Maize for seed production in CK was irrigated four times during the whole growth period and the other treatments were controlled by corresponding irrigation times with each irrigation quota 120 mm. Maize for seed production (*Zea mays* L. cv. Funong 963) was sown on April 15 and harvested on September 20, 2014. In 2015, the experiment consisted of seven irrigation treatments: One full irrigation treatment and six water deficit treatments (implemented by reducing the times of irrigation only at a specific stage). Full irrigation, irrigated four times during the whole growth season (CK); irrigated three times at the vegetative stage (IV3); irrigated three times at the reproductive stage (IR3); irrigated two times at the vegetative stage (IV2); irrigated two times at the reproductive stage (IR2); one irrigated time at the vegetative stage (IV1) and irrigated one time at the reproductive stage (IR1). Maize for seed production (*Zea mays* L. cv. Funong 588) was sown on April 15 and harvested on September 16, 2015. The experimental details of the second group of experiments were detailed in Ran et al. (2018). Maize was sown and harvested at the same date in both experiments. The soil surface was covered using 1.2 m-wide film sheet in the plant row with a 0.4 m-wide bare soil interval. In each experiment, the rate of Nitrogen (N), phosphorus (P_2O_5) and potassium (K_2O) fertilizers were 500, 240 and 50 kg ha^{-1}, respectively.

3.2. Calibration and validation procedures

The calibration and validation processes followed the steps below:

i Obtained transpiration of different irrigation treatments in Exp. 2 by adopting the output of the pre-calibrated AquaCrop model by Ran et al. (2018).

ii Calibrated WP^*_{KR-L} and WP^*_{KR-S} models by solving Eqs. (2) and (4) with measured biomass and ET data from EC system field in Exp. 1. To get the generic parameters, four year data were put together to calibrate the model (Fig. 2a). The B_m was set to 2000 g m^{-2} according to the average measured final biomass without water stress of Exp. 1. To abstract the WP^* model to a more generic form (standardized WP^*), both B_m and $\Sigma(T/ET_0)$ were standardized to 1 in each year from 2012 to 2015 (Fig. 2b). WP^*_{KR-L} and WP^*_{KR-S} models were validated using measured biomass data from Exp. 2. To apply the standardized WP^* models (WP^*_{KR-L} and WP^*_{KR-S}) to Exp. 2, the standardized $\Sigma(T/ET_0)$ [0, 1] was stretched to the actual $\Sigma(T/ET_0)$ of each treatment and the calculated biomass was multiplied by 2000 g m^{-2}. The simulated biomass by WP^*_{KR-L}, WP^*_{KR-S} and WP^*_{AC} models were compared with measured values to determine the optimal WP^* model.

iii Calibrated the HI_{KR-J}, HI_{KR-M}, HI_{KR-B} and HI_{KR-S} models using

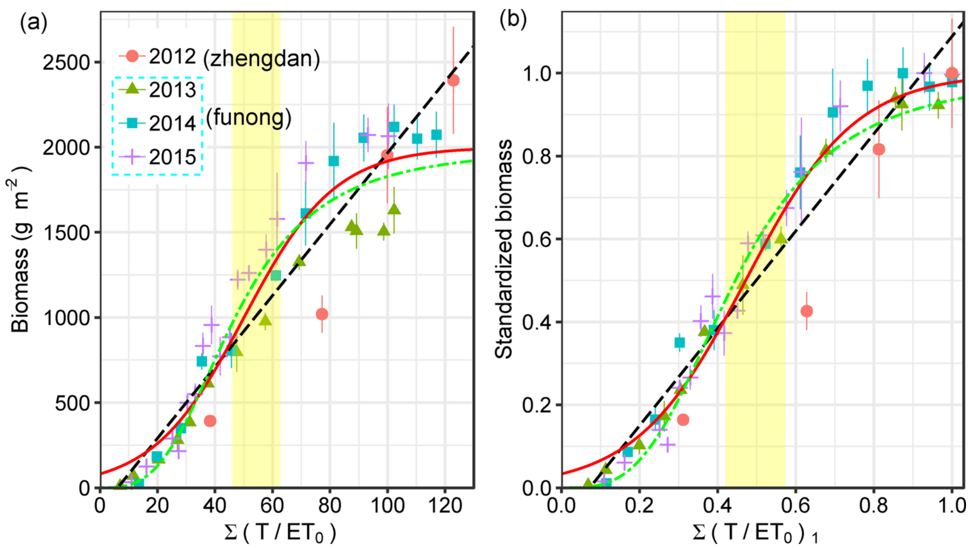

Fig. 2. (a) General regression between measured aboveground biomass and cumulative ratio of crop transpiration (T) to reference evapotranspiration (ET_0) during biomass measurement ($\Sigma(T/ET_0)$) and (b) standardized biomass and standardized $\Sigma(T/ET_0)$ ($\Sigma(T/ET_0)_1$) in a large field equipped with an eddy covariance (EC) system (Exp. 1) from 2012 to 2015. The points, red solid line, green dot-dashed line and black dashed line are measured values with error bars, fitted Logistic, Sigmoid and Linear equations, respectively. The light yellow band represents the flowering period. The varieties of 2012, 2013, 2014 and 2015 are Zhengdan 958, Funong 340, Funong 963 and Funong 588, respectively. The crop transpiration adopts EC measured evapotranspiration given transpiration is close to evapotranspiration as a result of over 70% of the surface covered by a film-mulch. (For interpretation of the references to colour in this figure legend, the reader is referred to the web version of this article).

Table 3
Parameters of new normalized water productivity (WP^*) and harvest index (HI) models for maize for seed production in Wuwei, Northwest China.

Model		Parameter	Description and unit	Value
WP^*	$WP^*_{KR\text{-}L}$	B_0	Initial biomass in $WP^*_{KR\text{-}L}$	0.033^{***} (66, g m^{-2}) (calibrated)
		δ	Potential biomass growth index in $WP^*_{KR\text{-}L}$	7.14^{***} (7.14) (calibrated)
	$WP^*_{KR\text{-}S}$	T_c	T^* value corresponding to half-maximum response in $WP^*_{KR\text{-}S}$	0.45^{***} (0.45) (calibrated)
		η	Constant in $WP^*_{KR\text{-}S}$	3.30^{***} (3.30) (calibrated)
		B_m	Potential final biomass without water stress in $WP^*_{KR\text{-}L}$ and $WP^*_{KR\text{-}S}$	1 (2000, g m^{-2}) (measured)
HI	$HI_{KR\text{-}J}$	ζ_1, ζ_2, ζ_3	Sensitivity index to water stress at vegetative, flowering and reproductive stage in $HI_{KR\text{-}J}$	0.10, 0.60^{**}, 0.22 (calibrated) (For yield: 0.5, 1.5, 0.5, Jensen et al., 1968; 0.29, 1.7, 0.54, Igbadun et al., 2007)
	$HI_{KR\text{-}M}$	μ_1, μ_2, μ_3	Sensitivity index to water stress at vegetative, flowering and reproductive stage in $HI_{KR\text{-}M}$	0.39, 1.06^{*}, 0.39 (calibrated) (For yield: 1.24, 3.36, 1.69, Igbadun et al., 2007)
	$HI_{KR\text{-}B}$	ε_1, ε_2, ε_3	Sensitivity coefficient to water stress at vegetative, flowering and reproductive stage in $HI_{KR\text{-}B}$	0.14, 0.80^{*}, 0.30 (calibrated) (For yield: 0.4, 1.5, 0.2-0.5, Doorenbos and Kassam, 1979; 0.21, 0.86, 0.49, Igbadun et al., 2007)
	$HI_{KR\text{-}S}$	ω_1, ω_2, ω_3	Sensitivity coefficient to water stress at vegetative, flowering and reproductive stage in $HI_{KR\text{-}S}$	0.11, 0.65^{**}, 0.24 (calibrated) (For yield: 0.35, 1.05, 0.2-0.4, Domínguez et al., 2012; 0.21, 0.86, 0.49, Igbadun et al., 2007)
		HI_m	Potential harvest index without water stress in $HI_{KR\text{-}J}$, $HI_{KR\text{-}M}$, $HI_{KR\text{-}B}$ and $HI_{KR\text{-}S}$, (%)	33 (measured)

$WP^*_{KR\text{-}L}$ and $WP^*_{KR\text{-}S}$ are non-linear dynamic normalized water productivity (WP^*) models derived using Logistic and Sigmiod equations, respectively. The calibrated value is for standardized WP^* with which final biomass and cumulative normalized crop transpiration are standardized to 1, and the number inside the brackets is the corresponding value for WP^*. $HI_{KR\text{-}J}$ and $HI_{KR\text{-}M}$ are new water deficit multiplicative-type HI models developed from Jensen and Minhas equations, respectively; $HI_{KR\text{-}B}$ and $HI_{KR\text{-}S}$ are new water deficit additive-type HI models developed from Blank and Stewart equations, respectively. T^* is the cumulative normalized crop transpiration ($\Sigma(T/ET_0)$).

*, ** and *** indicate significances at $P < 0.05$, $P < 0.01$ and $P < 0.001$ levels, respectively.

measured HI and transpiration outputted from the parameterized AquaCrop in Ran et al. (2018) in Exp. 2. The HI_m was set to 33% according to the average measured HI without water stress of Exp. 2. The sensitivity index or coefficient (ζ, μ, ε and ω) was restrained to a higher value within a more sensitive growth stage following the pattern in FAO 33 (Doorenbos and Kassam, 1979), i.e., flowering stage was noticed to be more sensitive than the other growth stages, followed by the reproductive stage and then the vegetative stage, for all the models (Doorenbos and Kassam, 1979; Igbadun et al., 2007; Domínguez et al., 2012). The validation of the new HI models adopted the approach of Leave-one-out cross validation (Jones and Carberry, 1994; Thorp et al., 2007), which required iterative and exhaustive four successive calibrations of the models by alternatively leaving out one year data. The simulated HI by $HI_{KR\text{-}J}$, $HI_{KR\text{-}M}$, $HI_{KR\text{-}B}$, $HI_{KR\text{-}S}$ and HI_{AC} models was compared with the measured values to determine the optimal HI model.

iv Multiplied final biomass outputted from the optimal WP^* model by HI outputted from the optimal HI model to get yield for AquaCrop-KR model. This was compared with the simulated yield by the original AquaCrop model in terms of the measured yield of Exp. 2.

3.3. Statistical analysis

The model parameters were fitted using the Nonlinear Least Squares Regression function in the R Programming Language. The accuracy of the models was quantified using the following criteria (Hsiao et al., 2009; Pereira et al., 2015; Ran et al., 2018):

$$b_0 = \frac{\sum_{i=1}^{n} M_i S_i}{\sum_{i=1}^{n} M_i^2}$$

$$R^2 = \left\{ \frac{\sum_{i=1}^{n} (M_i - \overline{M})(S_i - \overline{S})}{[\sum_{i=1}^{n} (M_i - \overline{M})^2]^{0.5} [\sum_{i=1}^{n} (S_i - \overline{S})^2]^{0.5}} \right\}^2$$

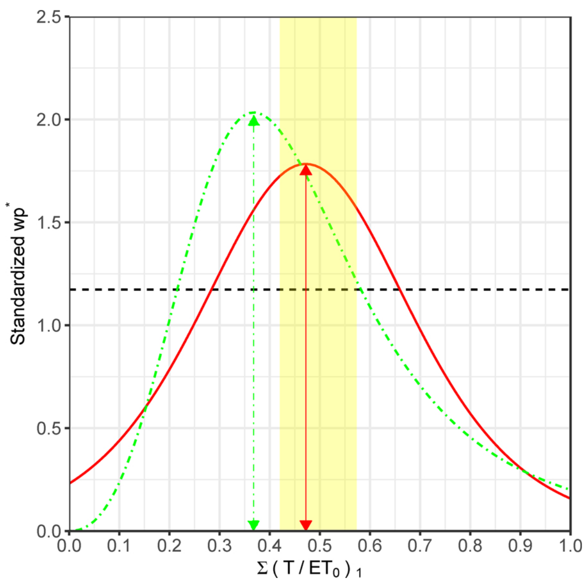

Fig. 3. Variation of standardized WP* of maize for seed production against normalized transpiration ($\Sigma(T/ET_0)_1$) from 2012 to 2015. The red solid line ($WP^*_{KR\text{-}L}$), green dot-dashed line ($WP^*_{KR\text{-}S}$) and black dashed line (WP^*_{AC}) are water productivity models derived using Logistic, Sigmiod and Linear equations, respectively. The light yellow band represents the flowering period. The arrow indicates the maximum of non-linear WP* model. T is crop transpiration, and ET_0 is reference evapotranspiration. The crop transpiration adopts EC measured evapotranspiration given transpiration is close to evapotranspiration as the result of over 70% film-mulch. (For interpretation of the references to colour in this figure legend, the reader is referred to the web version of this article).

Table 4
Basic characteristics for $WP^*_{KR\text{-}L}$ and $WP^*_{KR\text{-}S}$ models of maize for seed production during 2012–2015.

Model	Year	WP^*_{max}		IP1		IP2		GPL	
		DAP (d)	GDD (°C d)	DAP (d)	GDD (°C d)	DAP (d)	GDD (°C d)	DAP (d)	GDD (°C d)
$WP^*_{KR\text{-}L}$	2012	89	925	70	667	110	1212	155	1668
	2013	86	907	67	653	105	1162	145	1624
	2014	97	899	76	635	120	1168	159	1549
	2015	88	863	67	597	107	1114	155	1642
	Mean	90	899	70	638	111	1164	154	1621
$WP^*_{KR\text{-}S}$	2012	79	782	62	563	102	1103	155	1668
	2013	75	768	58	557	96	1044	145	1624
	2014	85	747	64	494	109	1052	159	1549
	2015	78	749	58	496	100	1011	155	1642
	Mean	79	762	61	527	102	1052	154	1621

$WP^*_{KR\text{-}L}$ and $WP^*_{KR\text{-}S}$ are non-linear dynamic normalized water productivity models derived using Logistic and Sigmiod equations, respectively. WP^*_{max} means the time to reach the maximum. IP1 and IP2 mean the first and the second intersection point where nonlinear models ($WP^*_{KR\text{-}L}$ and $WP^*_{KR\text{-}S}$) and linear model intersect, respectively. GPL is length of growth period. DAP is days after planting. GDD is growing degree days.

$$RMSE = \left[\frac{\sum_{i=1}^{n}(M_i - S_i)^2}{n}\right]^{0.5}$$

$$NRMSE = \frac{100}{\overline{M}}\left[\frac{\sum_{i=1}^{n}(M_i - S_i)^2}{n}\right]^{0.5}$$

$$EF = 1 - \frac{\sum_{i=1}^{n}(S_i - M_i)^2}{\sum_{i=1}^{n}(M_i - \overline{M})^2}$$

$$d = 1 - \frac{\sum_{i=1}^{n}(S_i - M_i)^2}{\sum_{i=1}^{n}(|S_i - \overline{M}| + |M_i - \overline{M}|)^2}$$

$$D = \frac{(S_i - M_i)}{M_i} \times 100$$

where S_i is the simulated values, M_i is the measured values, $\overline{S}$ is the mean of simulated values, and $\overline{M}$ is the mean of measured values. b_0 is the regression coefficient through the origin, and the simulated values are statistically close to the measured ones if b_0 is close to 1. R^2 is the coefficient of determination, and simulation results were considered acceptable if $R^2 > 0.5$ (Santhi et al., 2001). RMSE is root mean square error, and the errors between the simulated and measured values are small when RMSE is close to zero. NRMSE is normalized root mean square error, and the simulation is labeled excellent, good, fair and poor if the values of NRMSE are less than 10%, 10–20%, 20–30% and greater than 30%, respectively (Jamieson et al., 1991). EF is the Nash-Sutcliffe model efficiency coefficient, which ranges from minus infinity to 1; 1 means the exact match between the simulated and measured values, 0 indicates the same precision of simulated values and the average of measured values, and a negative number indicates the average of measured values is better than the simulated values. d is Willmott's index of agreement, which varies between 0 and 1; 0 means no agreement between the simulated and measured values, and 1 means exact agreement between the simulated and measured values. D is the relative error.

Mathematically, a model with more parameters would always be able to fit the data at least as well as a model with fewer parameters. To determine whether the nonlinear WP* model ($WP^*_{KR\text{-}L}$ and $WP^*_{KR\text{-}S}$, with more parameters) gave a significantly better fit to the data than the linear model (WP*, with less parameters), three approaches were used:

$$R^2_{adj} = 1 - (1 - R^2)\frac{n - 1}{n - \mathrm{k} - 1}$$

$$AIC = 2\mathrm{k} + n\ln\left(\frac{RSS}{n}\right)$$

$$F = \frac{\left(\frac{RSS_1 - RSS_2}{k_2 - k_1}\right)}{\left(\frac{RSS_2}{n - k_2}\right)}$$

where R^2_{adj} is adjusted R^2, which takes account of the number of parameters in a model (k) and the sample size (n) (https://en.wikipedia.org/wiki/Coefficient_of_determination#Adjusted_R2). The higher the R^2_{adj}, the better the model. AIC is Akaike information criterion, which is a goodness of fit to assess model accuracy and complexity. AIC favours smaller residual error in the model, but penalizes for more parameters. RSS is the residual sum of squares. The model is a better choice with a smaller AIC (Jin et al., 2017). F is the F-test. RSS_1 and RSS_2 are residual sum of squares of model 1 (with less parameters) and model 2 (with more parameters), respectively. k_1 and k_2 are the number of parameters in model 1 and model 2, respectively. If the calculated F is greater than the threshold value in the F distribution table with ($k_2 - k_1$, n-k_2) degrees of freedom, model 2 significantly better fits to the data than model 1 (https://en.wikipedia.org/wiki/F-test#Regression_problems).

4. Results

4.1. Model parameterization

When all four years of biomass data were analyzed together, the differences between Logistic, Sigmoid and Linear equations were not significant (Table 1). However, when both B_m and $\Sigma(T/ET_0)$ were standardized to 1, Logistic and Sigmoid equations were significantly better than Linear equation, and Logistic equation was the best (Table 1). The D of Logistic (-2.3%) and Sigmoid (−6.5%) for final biomass were smaller than the Linear equation (8.9%).

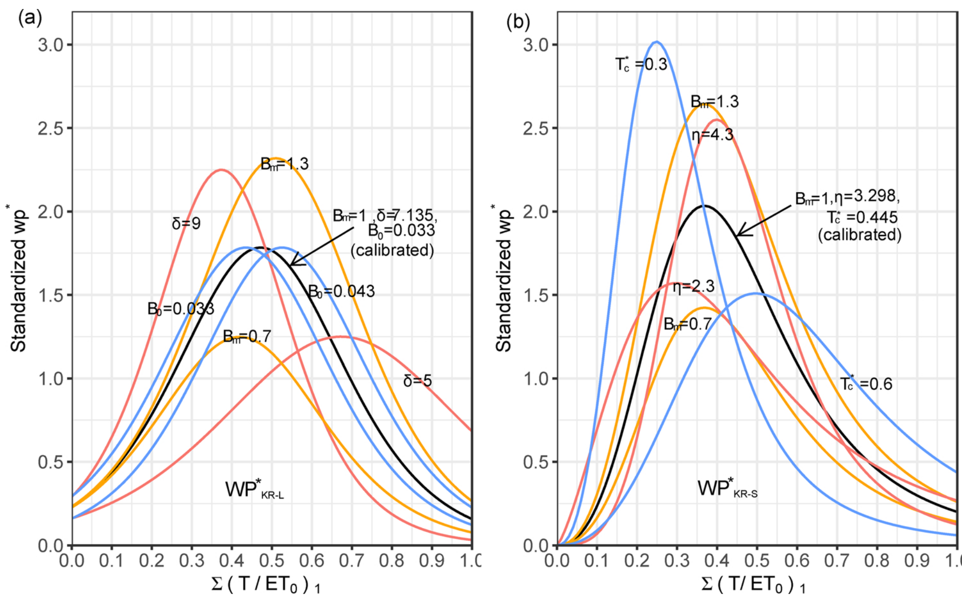

Fig. 4. Variation of $WP^*_{KR\text{-}L}$ and $WP^*_{KR\text{-}S}$ models with parameters changed. $WP^*_{KR\text{-}L}$ and $WP^*_{KR\text{-}S}$ are non-linear dynamic normalized water productivity models derived using Logistic and Sigmiod, respectively. The black line is normalized water productivity (WP^*) calibrated using measured data. The remain lines are corresponding WP^* when changing one parameter by ± 30% at a time. $\Sigma(T/ET_0)_1$ is standardized $\Sigma(T/ET_0)$. T is crop transpiration, and ET_0 is reference evapotranspiration.

Table 5

Statistical analysis of measured and simulated biomass process and final biomass (B) of maize for seed production under different irrigation treatments from the second group of experiments (Exp. 2) during 2012 to 2015.

	Model	Mean ($t\ ha^{-1}$)	n	b_0	R^2	RMSE ($t\ ha^{-1}$)	NRMSE (%)	EF	d
biomass	$WP^*_{KR\text{-}L}$	10.368	219	0.955	0.925	2.060	19.9	0.903	0.977
	$WP^*_{KR\text{-}S}$	10.368	219	0.970	0.926	2.011	19.4	0.907	0.978
	WP^*_{AC}	10.368	219	1.048	0.927	1.988	19.2	0.909	0.978
B	$WP^*_{KR\text{-}L}$	17.734	23	0.967	0.523	2.147	12.1	0.509	0.819
	$WP^*_{KR\text{-}S}$	17.734	23	0.960	0.559	2.093	11.8	0.533	0.822
	WP^*_{AC}	17.734	23	1.112	0.462	3.220	18.2	−0.104	0.697

n is number of samples. $WP^*_{KR\text{-}L}$ and $WP^*_{KR\text{-}S}$ are non-linear dynamic normalized water productivity models derived using Logistic and Sigmiod equations, respectively. WP^*_{AC} is normalized water productivity in AquaCrop model.

b_0 is the regression coefficient through the origin, R^2 is the determination coefficient, RMSE is the root mean square error, NRMSE is the normalized root mean square error, EF is the Nash-Sutcliffe model efficiency coefficient, and d is the Willmott's index of agreement. Measured biomass and simulated biomass by WP^*_{AC} are cited from Ran et al. (2018).

The parameters of the $WP^*_{KR\text{-}L}$ and $WP^*_{KR\text{-}S}$ models are showed in Table 3. The WP^* obtained by the linear model remained constant over the whole growth period, while the WP^* derived from the two "S" models (i.e. $WP^*_{KR\text{-}L}$ and $WP^*_{KR\text{-}S}$) showed a bell shape with the maximum value at $\Sigma(T/ET_0)_1$ of 0.37-0.47 (Fig. 3). The maximum value of the $WP^*_{KR\text{-}S}$ model was greater than that of the $WP^*_{KR\text{-}L}$ model. $WP^*_{KR\text{-}L}$ model reached its maximum at flowering stage (90 DAP, 899 °C d), and the time to reach the maximum value of $WP^*_{KR\text{-}S}$ was earlier (79 DAP, 762 °C d) (Fig. 3, Table 4). In addition, there were two intersection points between nonlinear models ($WP^*_{KR\text{-}L}$ and $WP^*_{KR\text{-}S}$) and the linear model (WP^*_{AC}). They were 0.283 and 0.659 for the first and the second intersection point between $WP^*_{KR\text{-}L}$ and WP^*_{AC} in $\Sigma(T/ET_0)_1$, corresponding to 70 (638) and 111 (1164) DAP (°C d). Between 70 and 111 DAP, the values of $WP^*_{KR\text{-}L}$ curve were greater than that of the WP^*_{AC} line, and the result was the opposite at the remaining days. For the first and the second intersection point between $WP^*_{KR\text{-}S}$ and WP^*_{AC}, they were 0.215 and 0.581 in $\Sigma(T/ET_0)_1$, corresponding to 61 (527) and 102 (1052) DAP (°C d). Between 61 and 102 DAP, the values of $WP^*_{KR\text{-}S}$ curve were greater than that of the WP^*_{AC} line, and the result was the opposite at the remaining days.

For both $WP^*_{KR\text{-}L}$ and $WP^*_{KR\text{-}S}$ models, parameter B_m controlled the size of the bell shape (Fig. 4). For $WP^*_{KR\text{-}L}$, the WP^* curve became sharp and narrow and the time to reach the maximum was advanced with higher δ. Parameter B_0 translated the curve. For $WP^*_{KR\text{-}S}$, the WP^* curve became sharp and narrow with the time to reach the maximum advanced with decreasing T^*_c. If increasing η, the curve became sharp and narrow with the time to reach the maximum delayed.

The relative HI (HI_a/HI_m) was significantly correlated with relative T (T_a/T_m) at the flowering stage (r = 0.80, $p < 0.001$), followed by T_a/T_m at the reproductive stage (r = 0.60, $p < 0.01$) and vegetative stage (r = 0.52, $p < 0.05$) (Table 2).The parameters of $HI_{KR\text{-}J}$, $HI_{KR\text{-}M}$, $HI_{KR\text{-}B}$ and $HI_{KR\text{-}S}$ models are showed in Table 3. The calibrated sensitivity index or coefficient at vegetative, flowering and reproductive stages in multiplicative-type or additive-type HI models were the similar to the pattern in Jensen et al. (1968), Doorenbos and Kassam (1979), Igbadun et al. (2007) and Domínguez et al. (2012). The parameters for the WP^* and HI sub-model in AquaCrop model were given by Ran et al. (2018).

4.2. Model validation

4.2.1. Biomass simulation

The "goodness of fit" of all the three models for biomass process was quite close (Table 5), however, the $WP^*_{KR\text{-}L}$ and $WP^*_{KR\text{-}S}$ models were better than the WP^*_{AC} model in simulating the variation of the biomass at maturity (Fig. 5). The simulated final biomass (B) by the $WP^*_{KR\text{-}L}$ and $WP^*_{KR\text{-}S}$ models were much closer to measured values than by WP^*_{AC} (Fig. 6), with NRMSE decreased to 12.1% and 11.8% from 18.2%, and EF increased to 0.509 and 0.533 from -0.104 (Table 5). For $WP^*_{KR\text{-}L}$ and WP^*_{AC}, the number of treatments having D of less than 5% were 7 and 4 (out of 23) (Table 9). Accordingly, the number of treatments having D of less than 15% were 18 and 12 (out of 23), less than 30% were 23 and 19 (out of 23), more than 30% were 0 and 4 (out of 23), and the

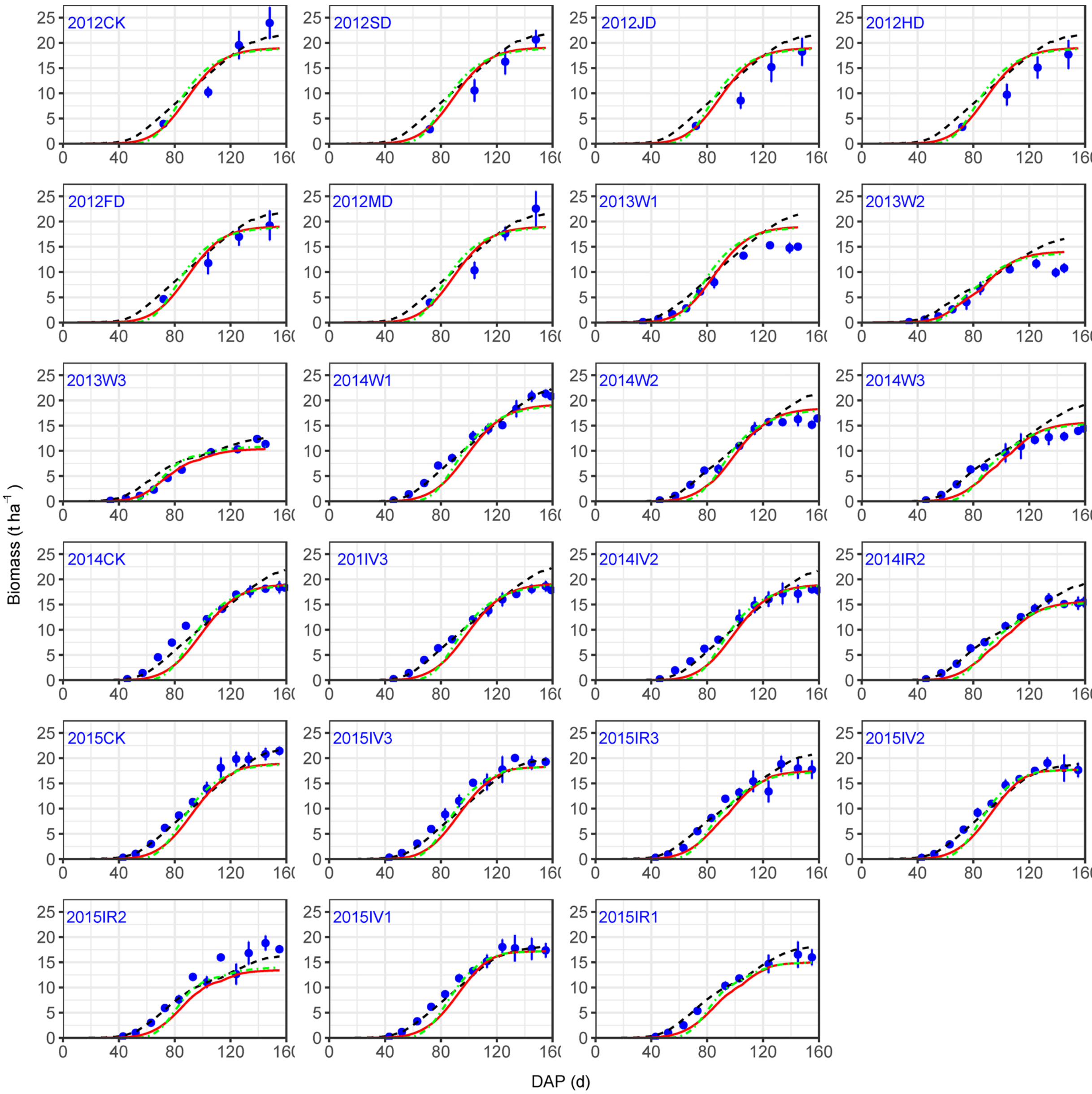

Fig. 5. Comparison of simulated biomass accumulation using $WP^{*}_{KR\text{-}L}$, $WP^{*}_{KR\text{-}S}$ and WP^{*}_{AC} models and measured values of maize for seed production under different irrigation treatments from the second group of experiments (Exp. 2) during 2012 to 2015. The red solid line, green dot dash line and black dashed line are simulated biomass using $WP^{*}_{KR\text{-}L}$, $WP^{*}_{KR\text{-}S}$ and WP^{*}_{AC} models, respectively. The blue dots are measured biomass with error bars. $WP^{*}_{KR\text{-}L}$ and $WP^{*}_{KR\text{-}S}$ are non-linear dynamic normalized water productivity models derived using Logistic and Sigmiod equations, respectively. WP^{*}_{AC} is the constant normalized water productivity in AquaCrop. DAP is days after planting. Measured biomass and simulated biomass by WP^{*}_{AC} are cited from Ran et al. (2018). (For interpretation of the references to colour in this figure legend, the reader is referred to the web version of this article).

maximum D were 29.6% and 53.6%, respectively. These results suggest that the $WP^{*}_{KR\text{-}L}$ model was better at simulating final biomass. Considering the calibration and validation results, $WP^{*}_{KR\text{-}L}$ was then used as the improved WP^{*} model for the yield simulation.

4.2.2. Harvest index simulation

The measured and simulated HI distributed near the 1:1 line for the $HI_{KR\text{-}J}$, $HI_{KR\text{-}M}$, $HI_{KR\text{-}B}$, and $HI_{KR\text{-}S}$ models (Fig. 7a–d), except for the HI_{AC} model, which significantly deviated from the 1:1 line (Fig. 7e). More importantly, all new HI models were more sensitive to water stress compared to the original HI_{AC} model, which remained constant under different irrigation conditions. For $HI_{KR\text{-}M}$ model b_0, R^2, RMSE, NRMSE, EF and d between the measured and simulated harvest index were 0.980, 0.555, 3.486%, 11.2%, 0.552 and 0.831, respectively, which were better than that for other HI modes (Table 6). The cross validation results proved the validity of the new developed HI models, with R^2 ranging from 0.514 to 0.577 and NRMSE ranging from 10.9% to 21.7% (Table 7). For $HI_{KR\text{-}M}$ and HI_{AC}, the treatment numbers with D of less than 5% were 7 and 6 (out of 23), respectively (Table 9). Accordingly, the treatment numbers with D of less than 15% were 20 and 17 (out of 23), less than 30% were 23 and 20 (out of 23), more than 30% were 0 and 3 (out of 23), and the maximum D were 24.3% and 94.3%, respectively (Table 9), indicating that the accuracy of the $HI_{KR\text{-}M}$ model was improved. Considering the above-mentioned evaluation indices, the newly developed $HI_{KR\text{-}J}$ and $HI_{KR\text{-}M}$, $HI_{KR\text{-}B}$ and $HI_{KR\text{-}S}$ models were successful, and the $HI_{KR\text{-}M}$ model was the best model, and was then used as the improved HI model for the yield simulation.

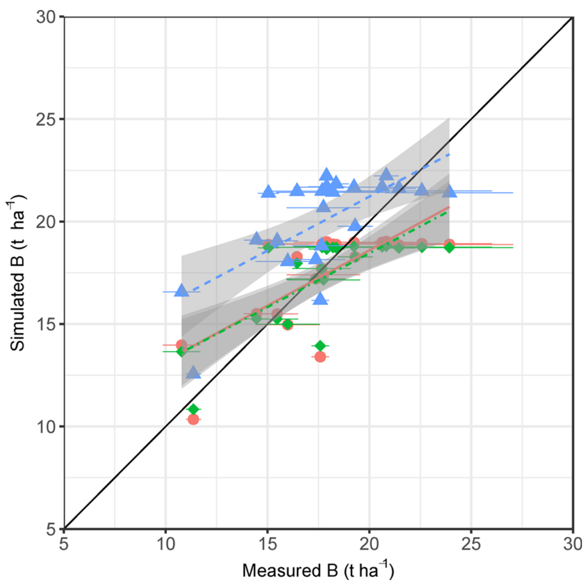

Fig. 6. Comparison of simulated final biomass (B) using $WP^*_{KR\text{-}L}$, $WP^*_{KR\text{-}S}$ and WP^*_{AC} models and measured values of maize for seed production under different irrigation treatments from the second group of experiments (Exp. 2) during 2012 to 2015. The red, green and blue dots are simulated B using $WP^*_{KR\text{-}L}$, $WP^*_{KR\text{-}S}$ and WP^*_{AC} models, respectively, and the corresponding colored lines with grey bands are trend lines with their 95% confidence intervals. $WP^*_{KR\text{-}L}$ and $WP^*_{KR\text{-}S}$ are non-linear dynamic normalized water productivity models derived using Logistic and Sigmiod equations, respectively. WP^*_{AC} is the constant normalized water productivity in AquaCrop. Measured and simulated B by WP^*_{AC} are cited from Ran et al. (2018). (For interpretation of the references to colour in this figure legend, the reader is referred to the web version of this article).

4.2.3. Yield simulation

The simulated and the measured yields were distributed near the 1:1 line for the AquaCrop-KR model (Fig. 8). In addition, when the measured yield was lower due to water stress, the simulated yield by the original AquaCrop model deviated from the 1:1 line, while the simulated yield by AquaCrop-KR remained near the 1:1 line (e.g., 2013W3), indicating that the AquaCrop-KR model owns the capability to simulate maize yield under different irrigation scenarios. For the AquaCrop-KR model the b_0, R^2, RMSE, NRMSE, EF and d between the measured and simulated yields were 0.950, 0.653, 0.901 t ha^{-1}, 16.1%, 0.642 and 0.881, respectively, which were better than that for the original AquaCrop model (Table 8), indicating that the simulated yield by AquaCrop-KR was closer to the measured value with smaller residuals. For the AquaCrop-KR and original AquaCrop models, the number of treatments having D of less than 5% were 7 and 7 (out of 23), respectively (Table 9). The number of treatments having D of less than 15% were 14 and 13, less than 30% were 19 and 16, more than 30% were 4 and 7. The maximum relative errors were 38.2% and 114.9%, respectively (Table 9), indicating that the AquaCrop-KR model had smaller simulation error.

5. Discussion

WP^* and HI are among the most sensitive of the parameters needed to simulate crop yield in AquaCrop (Razzaghi et al., 2017), due to their key role in determining biomass and yield development (Steduto et al., 2009; Ran et al., 2018). In the original AquaCrop model, WP^* is simplified to constant values for C3 (15-20 g m^{-2}) and C4 crops (30-35 g m^{-2}). This simplification greatly increases the ease use of the model, especially when data are not available for computing WP^*. However, the simplification also eliminates the essential characteristics of biomass accumulation with transpiration, which is characterized by the “S” shape (Fig. 1). The linear model balances the errors when the simulated biomass is overestimated and the errors when the simulated biomass is underestimated (Figs. 1, 2b). This is the reason why the linear model can simulate the biomass process overall with good accuracy, but the accuracy for final biomass is decreased (Figs. 5, 6, Table 5). In this study, the $WP^*_{KR\text{-}L}$ and $WP^*_{KR\text{-}S}$ models derived from the Logistic and Sigmoid functions captured the “S” shape characteristics of biomass accumulation versus transpiration, and improved the simulation of final biomass, which is the most important variable for decision making. It should be noted that small sample size of biomass measurements significantly weakened the superiority of the “S” shape models (Fig. 1a). If follow-up studies intend to reveal the variation of WP^*, the biomass sampling interval should be less than 10–15 days, because a larger interval will result in failing to capture the characteristics of biomass accumulation versus transpiration.

Many studies focus on the interannual variation of WP^* as water productivity is significantly affected by climate (Asseng and Hsiao, 2000; Steduto et al., 2007); however, few studies focus on the variation of WP^* within the growing season. This study demonstrates that WP^* varied within the growth season from mathematical and observational standpoints (Fig. 3). Usually, with increase of stomata opening, transpiration increase proportionally, whereas photosynthesis will saturate at certain point (Wang and Liu, 2003; Kang and Zhang, 2004). This suggests that the ratio between photosynthesis and transpiration, i.e. leaf scale water productivity, is not a constant. Chen (2015) studied the gross primary productivity (GPP), net ecosystem productivity (NEP) and ET with EC methods over maize for seed production under film drip irrigation at the same site of this study. They found that the ratio of GPP (or NEP) to the corresponding ET, i.e. canopy scale water productivity, is relatively low at early growth stages, increases during growth because the increment of photosynthetic rate is higher than that of ET (Bai et al., 2015), canopy scale water productivity reaches a maximum at mid-growth stage, then decreases during senescence (Appendix B, data unpublished). Stella et al. (2009) and Zhan et al. (2016) also found at similar pattern for the variation of canopy scale water productivity on maize with the EC technique. Zhao et al. (2007) and Bai et al. (2015) reported similar variation of water productivity at the canopy scale for winter wheat and cotton, respectively. These studies verify that water productivity varies within the growing season, in line with our results for WP^*. However, conventional view holds that biomass and water consumption are linearly related for the entire growing season, i.e. WP^* does not change (de Wit, 1958; Steduto, 2003; Steduto and Albrizio, 2005; Steduto et al., 2007). The underlying biochemical processes conveying informations about enzymatic activity might helps to interpret the variation of WP^* during growth period, but are beyond the scope of our study.

One crucially important parameter in the newly developed $WP^*_{KR\text{-}L}$ and $WP^*_{KR\text{-}S}$ models is B_m, which owns definite physiological meaning, and should be a constant for a specific variety. B_m should be carefully assigned, because it directly determines the maximum scope of the simulated biomass. Although the new WP^* models are more complex than the linear model, the parameters are relatively easy to obtain, especially for B_m, which is easy to get through field data, published literature or farmers' experience. Crops might also be grouped in classes having a similar B_m, which helps to adopt similar $WP^*_{KR\text{-}L}$ (or $WP^*_{KR\text{-}S}$) curves for different crops. Abstracting the relationship between measured biomass and transpiration in maize on light sandy loam soil in arid inland climate (Fig. 2a) to a mathematical equation with physiological parameters (Fig. 2b) facilitates the application of the new WP^* model in other kind of herbaceous crops, types of climate, soils, and drought by stretching the shape of standardized WP^* curve in Fig. 3. When applying the $WP^*_{KR\text{-}L}$ (or $WP^*_{KR\text{-}S}$) model, the cumulative normalized T ($\Sigma(T/ET_0)$) on the abscissa is actually similar to the DAP or GDD, representing the phenology. If due to water stress, the $\Sigma(T/ET_0)$ is lower than the potential $\Sigma(T/ET_0)$, then $\Sigma(T/ET_0)$ in $WP^*_{KR\text{-}L}$ (or $WP^*_{KR\text{-}S}$) curve is automatically stretched to match the actual $\Sigma(T/ET_0)$, i.e. the actual pattern of the curve is kept. This is also the reason why we

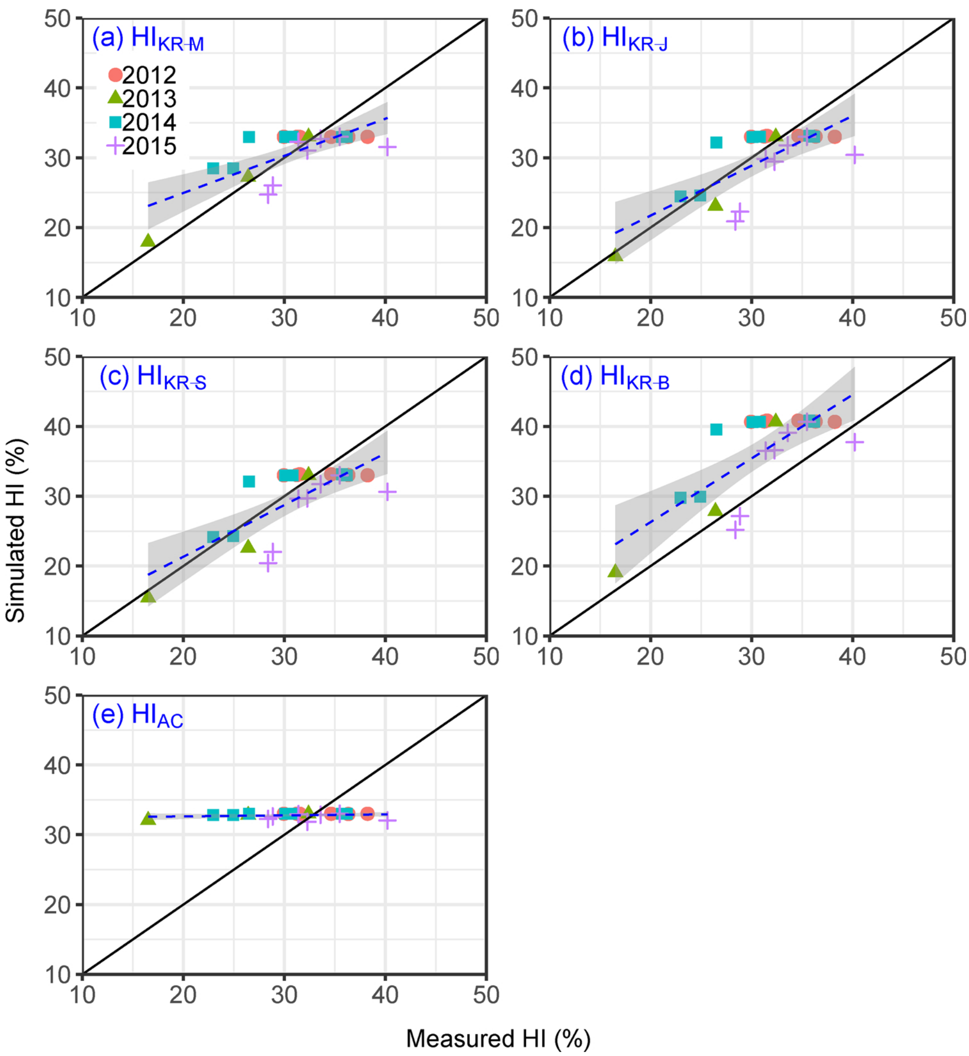

Fig. 7. Comparison of measured and simulated harvest index (HI) of maize for seed production under different irrigation treatments from the second group of experiments (Exp. 2) from 2012 to 2015. The blue dashed lines with grey bands are trend lines with 95% confidence intervals. HI_{KR-J} and HI_{KR-M} are new water deficit multiplicative-type HI models developed from Jensen and Minhas equations, respectively; HI_{KR-B} and HI_{KR-S} are new water deficit additive-type HI models developed from Blank and Stewart equations, respectively. HI_{AC} is the sub-HI model in the AquaCrop model. Measured HI and simulated HI by the HI_{AC} model are cited from Ran et al. (2018). (For interpretation of the references to colour in this figure legend, the reader is referred to the web version of this article).

Table 6

Statistical analysis of the parameterized harvest index (HI) models for maize for seed production under different irrigation treatments from the second group of experiments (Exp. 2) during 2012 to 2015.

Rank	Model	Mean (%)	n	b_0	R^2	RMSE (%)	NRMSE (%)	EF	d
1	HI_{KR-M}	31.1	23	0.980	0.555	3.486	11.2	0.552	0.831
2	HI_{KR-J}	31.1	23	0.947	0.562	3.885	12.5	0.443	0.842
3	HI_{KR-S}	31.1	23	0.945	0.569	3.931	12.7	0.430	0.843
4	HI_{KR-B}	31.1	23	1.164	0.569	6.752	21.7	−0.681	0.706
5	HI_{AC}	31.1	23	1.027	0.046	5.423	17.5	−0.084	0.312

HI_{KR-J} and HI_{KR-M} are new water deficit multiplicative-type HI models developed from Jensen and Minhas equations, respectively; HI_{KR-B} and HI_{KR-S} are new water deficit additive-type HI models developed from Blank and Stewart equations, respectively. HI_{AC} is the sub-HI model in the AquaCrop model.
n is the number of samples. b_0 is the regression coefficient through the origin, R^2 is the determination coefficient, RMSE is the root mean square error, NRMSE is the normalized root mean square error, EF is the Nash-Sutcliffe model efficiency coefficient, and d the is Willmott's index of agreement. Measured HI and simulated HI by HI_{AC} model are cited from Ran et al. (2018).

standardize $\Sigma(T/ET_0)$ to [0, 1] $(\Sigma(T/ET_0)_1)$ for a more generic form. Thus the WP^*_{KR-L} (or WP^*_{KR-S}) model will not overestimate biomass under water stress conditions compared to a linear model (e.g., Fig. 5 2013w3), because each water stress treatment will undergo a complete WP^*_{KR-L} (or WP^*_{KR-S}) curve. Furthermore, for crops with yield that are rich in lipids or proteins, AquaCrop adopts two different values for the pre-anthesis and post-anthesis WP^* because more energy is required than for the synthesis of carbohydrates (Azam-Ali and Squire, 2002). This study provides a non-linear dynamic WP^* model calculating WP^* value at a daily scale, which might be applied to different types of crops with different levels of carbohydrates, lipids and proteins by adjusting corresponding B_m.

Four HI models: HI_{KR-J} and HI_{KR-M}, which are multiplicative models, and HI_{KR-B} and HI_{KR-S}, which are additive models, are evaluated. The multiplicative-type HI models imply that HI will be zero if there is no transpiration in any growth stage while the additive-type HI models mean that lack of transpiration at any growth stage may not necessarily lead HI to zero but could severely decrease HI. By comparing with the measured HI under different water stress conditions, the newly established harvest index models show good simulation results (Fig. 7). This indicates that the hypothesis of developing the relationship between HI and crop transpiration using the form of crop water production functions is feasible. Crop transpiration is a more intrinsic indicator to reflect water stress than soil water content (e.g. Denmead and Shaw, 1962).

All the parameters in the new HI models are physiologically meaningful. HI_m is the ratio of the yield to the total aboveground biomass that will be reached at maturity for non-stressed conditions, which is a conservative cultivar-specific parameter. HI_m should be carefully identified, because the uncertainty of HI_m will bring systematic overestimation or underestimation of actual HI for all treatments. The

Table 7
Validation of the four new harvest index (HI) models on maize for seed production under different irrigation treatments from the second group of experiments (Exp. 2) during 2012 to 2015 with leave-one-out cross validation approach.

Models	Calibration				Validation			
	Year	n	R^2	NRMSE (%)	Year	n	R^2	NRMSE (%)
HI_{KR-J}	2013, 2014, 2015	17	0.575	13.7	2012	6	0.020	9.0
	2012, 2014, 2015	20	0.339	12.8	2013	3	0.936	9.1
	2012, 2013, 2015	16	0.632	13.3	2014	7	0.627	10.2
	2012, 2013, 2014	16	0.736	9.5	2015	7	0.541	16.9
	Mean		0.571	12.3			0.531	11.3
HI_{KR-M}	2013, 2014, 2015	17	0.567	12.0	2012	6	0.019	9.1
	2012, 2014, 2015	20	0.269	11.6	2013	3	0.999	8.2
	2012, 2013, 2015	16	0.691	9.9	2014	7	0.573	14.4
	2012, 2013, 2014	16	0.693	10.2	2015	7	0.466	14.5
	Mean		0.555	10.9			0.514	11.6
HI_{KR-B}	2013, 2014, 2015	17	0.583	21.2	2012	6	0.020	22.8
	2012, 2014, 2015	20	0.344	21.8	2013	3	0.939	20.2
	2012, 2013, 2015	16	0.638	18.5	2014	7	0.630	28.4
	2012, 2013, 2014	16	0.734	25.1	2015	7	0.556	12.7
	Mean		0.575	21.7			0.536	21.0
HI_{KR-S}	2013, 2014, 2015	17	0.583	13.9	2012	6	0.020	9.0
	2012, 2014, 2015	20	0.352	12.8	2013	3	0.924	11.0
	2012, 2013, 2015	16	0.638	13.5	2014	7	0.630	10.1
	2012, 2013, 2014	16	0.734	9.6	2015	7	0.556	17.1
	Mean		0.577	12.5			0.533	11.8

HI_{KR-J} and HI_{KR-M} are new water deficit multiplicative-type HI models developed from Jensen and Minhas equations, respectively; HI_{KR-B} and HI_{KR-S} are new water deficit additive-type HI models developed from Blank and Stewart equations, respectively. n is number of samples. R^2 is the determination coefficient, and NRMSE is the normalized root mean square error.

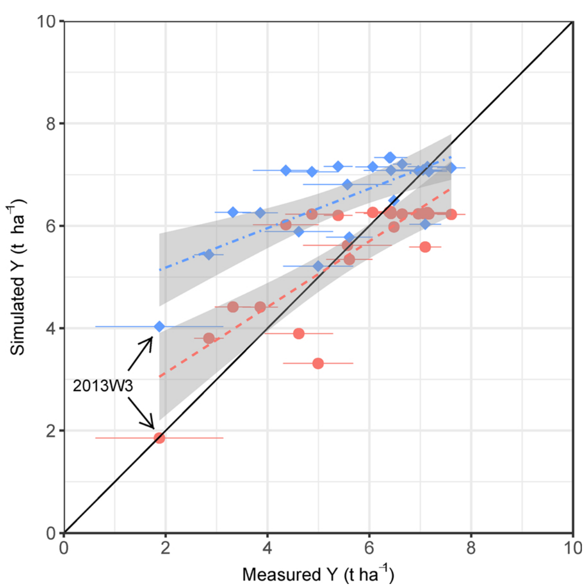

Fig. 8. Comparison of measured and simulated yield (Y) of maize for seed production under different irrigation treatments from the second group of experiments (Exp. 2) from 2012 to 2015. The red and blue dots are simulated Y using AquaCrop-KR and AquaCrop, respectively, and the corresponding colored lines with grey bands are trend lines with their 95% confidence intervals. 2013W3 represents the most severe water stress treatment. AquaCrop-KR means yields calculated based on WP^*_{KR-L} and HI_{KR-M} models. WP^*_{KR-L} is a non-linear dynamic normalized water productivity model derived using the Logistic equation. HI_{KR-M} is a water deficit multiplicative harvest index model developed using the Minhas equation. Measured Y and simulated Y by AquaCrop are cited from Ran et al. (2018). (For interpretation of the references to colour in this figure legend, the reader is referred to the web version of this article).

Table 8
Statistical analysis of measured and simulated yield (Y) of maize for seed production under different irrigation treatments from the second group of experiments (Exp. 2) during 2012–2015.

Models	Mean (t ha^{-1})	n	b_0	R^2	RMSE (t ha^{-1})	NRMSE (%)	EF	d
AquaCrop-KR	5.598	23	0.950	0.653	0.901	16.1	0.642	0.881
AquaCrop	5.598	23	1.120	0.496	1.466	26.2	0.055	0.681

AquaCrop-KR is the yield calculation model based on WP^*_{KR-L} and HI_{KR-M}. WP^*_{KR-L} is non-linear dynamic normalized water productivity models derived using the Logistic equation. HI_{KR-M} is a water deficit multiplicative harvest index model developed based on the Minhas equation. Measured yield and simulated yield by AquaCrop are cited from Ran et al. (2018).
n is the number of samples. b_0 is the regression coefficient through the origin, R^2 is the determination coefficient, RMSE is the root mean square error, NRMSE is the normalized root mean square error, EF is the Nash-Sutcliffe model efficiency coefficient, and d is the Willmott's index of agreement.

sensitivity index or coefficient (ζ, μ, ε and ω) captures the essence of the complex linkages between HI and water stress, where many biophysical processes are involved (e.g. Andersen et al., 2002). It seems feasible to calibrate ζ, μ, ε and ω following the pattern in FAO 33 in this study (Fig. 7; Table 7), however, only the fitted $ζ_2$, $μ_2$, $ε_2$ and $ω_2$ at the flowering stage are significant and ζ, μ, ε and ω at the other two stages are not significant (Table 3). This indicates that ζ, μ, ε and ω at the vegetative and reproductive growth carry more uncertainties, and need more measured data to justify. The calibrated ζ, μ, ε and ω in new HI models are lower than the reference value in crop water production functions (Table 3). This fact may be justified because water stress also decreases biomass which also brings loss in Y. No other comparisons for ζ, μ, ε and ω are made due to a lack of similar studies on HI. Considering the limited data and treatments in this study, the ζ, μ, ε and ω in the four HI models need to be further calibrated and validated under longer time series and more irrigation scenarios. Moreover, the four new HI models should be improved in future studies. For example, this study does not distinguish the transpiration of male and female parents. The accuracy of the developed HI models may be more accurate if considering the transpiration of the male parent before the end of pollination and the transpiration of the female parent over the whole growth period.

The main objective of this study is to share some new alternative possibilities and models for simulating WP^* and HI under stress condition in arid regions, which has potential for application to other kind of herbaceous crops, type of climate, soil types, and abiotic stresses. The developed HI model is proposed as a method to estimate yield in conjunction with a WP^*-based method to simulate biomass production. The combination results in a yield model entirely based on crop transpiration. This confirms that the crop transpiration can be used as a driving factor for yield simulation. In comparison to the original AquaCrop model, AquaCrop-KR based on WP^*_{KR-L} and HI_{KR-M} models decreases the error in yield simulation (Fig. 8). It strongly suggests that the newly developed WP^* and HI models are helpful modifications for improving yield simulation, especially for severe water stress conditions. However, the newly developed WP^* models increased the number of parameters, and the sensitivity index (coefficient) in newly HI models need sufficient data including various irrigation treatments to be calibrated correctly. If enough data are available to obtain these parameters, we propose to adopt the new WP^* and HI models. Otherwise, the original AquaCrop is recommended, given it has acceptable performance and needs fewer parameters (Hsiao et al., 2009; Heng et al., 2009; Ran et al., 2018).

Table 9
Comparison of measured and simulated final biomass (B), harvest index (HI) and yield (Y) of maize for seed production with the AquaCrop-KR and original AquaCrop models under different irrigation treatments from the second group of experiments (Exp. 2) during 2012–2015.

Year	Treatment	B_{mea} (t ha^{-1})	$B_{KR\text{-}L}$ (t ha^{-1})	D (%)	B_{AC} (t ha^{-1})	D (%)	HI_{mea} (%)	$HI_{KR\text{-}M}$ (%)	D (%)	HI_{AC} (%)	D (%)	Y_{mea} (t ha^{-1})	$Y_{AC\text{-}KR}$ (t ha^{-1})	D (%)	Y_{AC} (t ha^{-1})	D (%)
2012	CK	23.928	18.881	−21.1	21.399	−10.6	30.0	33.0	10.2	33.0	10.2	7.167	6.231	−13.1	7.062	−1.5
	SD	20.621	18.980	−8.0	21.680	5.1	34.6	33.0	−4.8	33.0	−4.7	7.141	6.259	−12.3	7.155	0.2
	JD	18.208	18.894	3.8	21.428	17.7	38.2	33.0	−13.7	33.0	−13.7	6.961	6.235	−10.4	7.071	1.6
	HD	17.680	18.910	7.0	21.483	21.5	36.3	33.0	−9.2	33.0	−9.2	6.424	6.240	−2.9	7.084	10.3
	FD	19.244	18.985	−1.3	21.674	12.6	31.5	33.0	4.6	33.0	4.7	6.066	6.261	3.2	7.153	17.9
	MD	22.576	18.916	−16.2	21.490	−4.8	31.2	33.0	5.6	33.0	5.6	7.054	6.242	−11.5	7.092	0.5
2013	W1	15.041	18.876	25.5	21.384	42.2	32.4	33.0	1.9	33.0	1.9	4.871	6.229	27.9	7.056	44.9
	W2	10.780	13.970	29.6	16.563	53.6	26.4	27.2	3.1	32.8	24.3	2.848	3.803	33.5	5.438	91.0
	W3	11.357	10.348	−8.9	12.565	10.6	16.5	17.9	8.5	32.1	94.3	1.876	1.854	−1.1	4.033	114.9
2014	W1	20.828	19.028	−8.6	22.231	6.7	30.8	33.0	7.1	33.0	7.1	6.418	6.279	−2.2	7.336	14.3
	W2	16.446	18.280	11.2	21.470	30.5	26.5	32.9	24.3	33.0	24.4	4.359	6.022	38.2	7.082	62.5
	W3	14.459	15.505	7.2	19.096	32.1	23.0	28.5	24.0	32.8	42.9	3.320	4.415	33.0	6.265	88.7
	CK	18.364	18.877	2.8	21.839	18.9	36.2	33.0	−8.8	33.0	−8.8	6.643	6.229	−6.2	7.207	8.5
	IV3	17.894	19.009	6.2	22.217	24.2	35.7	33.0	−7.6	33.0	−7.6	6.389	6.269	−1.9	7.331	14.7
	IV2	17.900	18.807	5.1	21.698	21.2	30.1	33.0	9.6	33.0	9.7	5.386	6.204	15.2	7.160	32.9
	IR2	15.471	15.490	0.1	19.060	23.2	24.9	28.5	14.3	32.8	31.7	3.855	4.413	14.5	6.253	62.2
2015	CK	21.447	18.854	−12.1	21.613	0.8	35.5	33.0	−7.0	33.0	−7.0	7.608	6.222	−18.2	7.132	−6.3
	IV3	19.299	18.276	−5.3	19.765	2.4	33.6	32.7	−2.6	32.9	−2.2	6.481	5.978	−7.8	6.494	0.2
	IR3	17.744	17.402	−1.9	20.674	16.5	31.4	32.3	2.9	32.9	4.9	5.569	5.618	0.9	6.807	22.2
	IV2	17.653	17.712	0.3	18.819	6.6	40.2	31.5	−21.5	32.1	−20.3	7.096	5.587	−21.3	6.032	−15.0
	IR2	17.587	13.400	−23.8	16.157	−8.1	28.4	24.7	−13.0	32.3	13.6	4.993	3.312	−33.7	5.213	4.4
	IV1	17.371	17.211	−0.9	18.139	4.4	32.3	31.0	−3.8	31.9	−1.3	5.606	5.343	−4.7	5.778	3.1
	IR1	15.990	14.964	−6.4	18.052	12.9	28.9	26.0	−9.8	32.6	13.0	4.613	3.895	−15.6	5.887	27.6

$B_{KR\text{-}L}$ is the calculated B based on $WP^*_{KR\text{-}L}$ model. $HI_{KR\text{-}M}$ is the calculated HI based on the $HI_{KR\text{-}M}$ model. $Y_{AC\text{-}KR}$ is the calculated yield based on AquaCrop-KR with the $WP^*_{KR\text{-}L}$ and $HI_{KR\text{-}M}$ models. $WP^*_{KR\text{-}L}$ is a non-linear dynamic normalized water productivity models derived using Logistic equation. $HI_{KR\text{-}M}$ is a water deficit multiplicative harvest index model developed based on the Minhas equation. The subscript 'mea' refers to measured values, and D is the relative error. Measured B, HI and Y and their simulations by AquaCrop are cited from Ran et al. (2018).

6. Conclusions

The newly developed $WP^*_{KR\text{-}L}$ model improved the simulation accuracy of biomass, especially for the final biomass. The newly developed $HI_{KR\text{-}M}$ model was more sensitive to water stress than the HI submodel of the original AquaCrop model. The accuracy of yield was higher when calculated based on the $WP^*_{KR\text{-}L}$ and $HI_{KR\text{-}M}$ models. Therefore, the $WP^*_{KR\text{-}L}$ and the $HI_{KR\text{-}M}$ models can be recommended for simulating the biomass and harvest index, and should be tested in other crops and regions. The newly established $WP^*_{KR\text{-}L}$ and $HI_{KR\text{-}M}$ models are driven by crop transpiration, indicating that crop transpiration can be used as a driving factor for yield simulation in the future.

Acknowledgements

We appreciate the assistance of Jinliang Chen from Institut National de la Recherche Agronomique, INRA, France, and Jintao Wang from Institute of Genetics and Developmental Biology, CAS, China. We are also grateful to the anonymous reviewers and editors for their work on this manuscript. This research was financially supported by the National Natural Science Foundation of China (grants 51809216, 51790534 and 51621061), the Government Public Research Funds for Projects of the Ministry of Agriculture (201503125), the Discipline Innovative Engineering Plan (111 Program, B14002) and the Fundamental Research Funds for the Central Universities (2452017203).

Appendix A

Mathematical derivation process of $WP^*_{KR\text{-}L}$ and $WP^*_{KR\text{-}S}$ from Logistic and Sigmoid equation.

$$
\begin{aligned}
WP^*_{KR-L} &= \frac{dB_t}{dT^*} \\
&= -B_m B_0 \frac{1}{[B_0 + (B_m - B_0)e^{-\delta T^*}]^2}[B_0 + (B_m - B_0)e^{-\delta T^*}]' \\
&= -B_m B_0 \frac{1}{[B_0 + (B_m - B_0)e^{-\delta T^*}]^2}(B_m - B_0)(e^{-\delta T^*})' \\
&= -B_m B_0 \frac{1}{[B_0 + (B_m - B_0)e^{-\delta T^*}]^2}(B_m - B_0)(-\delta)e^{-\delta T^*} \\
&= \frac{B_m B_0 \delta (B_m - B_0)e^{-\delta T^*}}{[B_0 + (B_m - B_0)e^{-\delta T^*}]^2}
\end{aligned}
$$

$$
\begin{aligned}
WP^{*}_{KR-S} &= \frac{dB_t}{dT^{*}} \\
&= \frac{d}{dT^{*}}\left[\frac{B_{\mathrm{m}}T^{*\eta}}{T_c^{\eta}+T^{*\eta}}\right] \\
&= B_m\frac{(T^{*\eta})'(T_c^{\eta}+T^{*\eta})-T^{*\eta}(T_c^{\eta}+T^{*\eta})'}{(T_c^{\eta}+T^{*\eta})^2} \\
&= B_m\frac{\eta T^{*\eta-1}(T_c^{\eta}+T^{*\eta})-T^{*\eta}\eta T^{*\eta-1}}{(T_c^{\eta}+T^{*\eta})^2} \\
&= \frac{\eta B_m T_c^{\eta}T^{*\eta-1}}{(T_c^{\eta}+T^{*\eta})^2}
\end{aligned}
$$

Appendix B

Seasonal variations of water use efficiency (WUE) on gross primary productivity (GPP) (a) and net ecosystem productivity (NEP) levels (b) for maize for seed production from sowing to maturing under film drip irrigation in 2014 in Northwest China. Cited from Chen (2015).

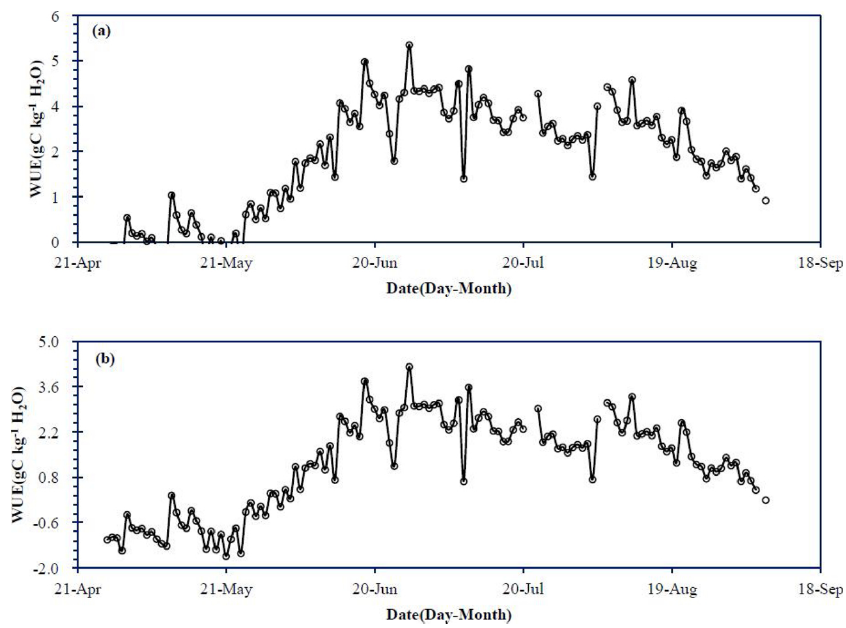

References

Abedinpour, M., Sarangi, A., Rajput, T.B.S., Singh, M., Pathak, H., Ahmad, T., 2012. Performance evaluation of AquaCrop model for maize crop in a semi-arid environment. Agric. Water Manag. 110, 55–66.

Allen, R.G., Pereira, L.S., Raes, D., Smith, M., 1998. Crop Evapotranspiration. Guidelines for Computing Crop Water Requirements. FAO Irrigation and Drainage Paper 56. FAO, Rome, Italy 300p.

Andarzian, B., Bannayan, M., Steduto, P., Mazraeh, H., Barati, M.E., Barati, M.A., Rahnama, A., 2011. Validation and testing of the AquaCrop model under full and deficit irrigated wheat production in Iran. Agric. Water Manag. 100 (1), 1–8.

Andersen, M.N., Asch, F., Wu, Y., Jensen, C.R., Næsted, H., Mogensen, V.O., Koch, K.E., 2002. Soluble invertase expression is an early target of drought stress during the critical, abortion-sensitive phase of young ovary development in maize. Plant Physiol. 130, 591–604.

Araya, A., Habtu, S., Hadgu, K.M., Kebede, A., Dejene, T., 2010. Test of AquaCrop model in simulating biomass and yield of water deficient and irrigated barley (Hordeum vulgare). Agric. Water Manag. 97 (11), 1838–1846.

Asseng, S., Hsiao, T.C., 2000. Canopy CO_2 assimilation, energy balance, and water use efficiency of an alfalfa crop before and after cutting. Field Crops Res. 67, 191–206.

Azam-Ali, S.N., Squire, G.R., 2002. Principles of Tropical Agronomy. CABI Publishing, Wallingford, UK.

Bai, J., Wang, J., Chen, X., Luo, G., Shi, H., Li, L., Li, J., 2015. Seasonal and inter-annual variations in carbon fluxes and evapotranspiration over cotton field under drip irrigation with plastic mulch in an arid region of Northwest China. J. Arid Land 7 (2), 272–284.

Balwinder, S., Eberbach, P.L., Humphreys, E., Kukal, S.S., 2011. The effect of rice straw mulch on evapotranspiration, transpiration and soil evaporation of irrigated wheat in Punjab, India. Agric. Water Manag. 98 (12), 1847–1855.

Blank, H., 1975. Optimal Irrigation Decisions with Limited Water. Master Thesis. Colorado State University, Fort Collins.

Bolaños, J., Edmeades, G., 1993. Eight cycles of selection for drought tolerance in lowland tropical maize. I. Responses in grain yield, biomass, and radiation utilization. Field Crops Res. 31 (3-4), 233–252.

Chen, X., 2015. The Study on the Exchange of Carbon of Maize under Film Drip Irrigation in Arid Regions of Northwest China. Master Thesis. China Agricultural University, Beijing in Chinese, with English abstract.

de Wit, C.T., 1958. Transpiration and Crop Yields. Wageningen University, Wageningen, The Netherlands, pp. 1–88.

DeLougherty, R.L., Crookston, R.K., 1979. Harvest index of corn affected by population density, maturity rating, and environment. Agron. J. 71 (4), 577–580.

Denmead, O.T., Shaw, R.H., 1962. Availability of soil water to plants as affected by soil moisture content and meteorological conditions. Agron. J. 54, 385–390.

Ding, R., Kang, S., Li, F., Zhang, Y., Tong, L., Sun, Q., 2010. Evaluating eddy covariance method by large-scale weighing lysimeter in a maize field of northwest China. Agric. Water Manag. 98 (1), 87–95.

Domínguez, A., Martinez, R.S., de Juan, J.A., Martinez-Romero, A., Tarjuelo, J.M., 2012. Simulation of maize crop behavior under deficit irrigation using MOPECO model in a semi-arid environment. Agric. Water Manag. 107, 42–53.

Doorenbos, J., Kassam, A.H., 1979. Yield Response to Water. FAO Irrigation and Drainage Paper 33. FAO, Rome, Italy 193p.

Farahani, H.J., Izzi, G., Oweis, T.Y., 2009. Parameterization and evaluation of the AquaCrop model for full and deficit irrigated cotton. Agron. J. 101 (3), 469–476.

Farré, I., Faci, J.M., 2006. Comparative response of maize (Zea mays L.) and sorghum (Sorghum bicolor L. Moench) to deficit irrigation in a Mediterranean environment. Agric. Water Manag. 83 (1), 135–143.

Heng, L.K., Hsiao, T., Evett, S., Howell, T., Steduto, P., 2009. Validating the FAO AquaCrop model for irrigated and water deficient field maize. Agron. J. 101 (3), 488–498.

Hsiao, T.C., Heng, L., Steduto, P., Rojas-Lara, B., Raes, D., Fereres, E., 2009. AquaCrop—the FAO crop model to simulate yield response to water: III. Parameterization and testing for maize. Agron. J. 101 (3), 448–459.

Igbadun, H.E., Tarimo, A., Salim, B.A., Mahoo, H.F., 2007. Evaluation of selected crop

water production functions for an irrigated maize crop. Agric. Water Manag. 94 (1-3), 1–10.
Jamieson, P.D., Porter, J.R., Wilson, D.R., 1991. A test of computer simulation model ARC-WHEAT1 on wheat crops grown in New Zealand. Field Crops Res. 27, 337–350.
Jensen, M.E., 1968. Water consumption by agricultural plants. In: In: Kozlowski, T.T. (Ed.), Water Deficits and Plant Growth Vol. 2. Academic Press, New York, pp. 1–22.
Jiang, X., Kang, S., Li, F., Du, T., Tong, L., Comas, L., 2016a. Evapotranspiration partitioning and variation of sap flow in female and male parents of maize for hybrid seed production in arid region. Agric. Water Manag. 176, 132–141.
Jiang, X., Kang, S., Tong, L., Li, F., 2016b. Modification of evapotranspiration model based on effective resistance to estimate evapotranspiration of maize for seed production in an arid region of northwest China. J. Hydrol. 538, 194–207.
Jin, X., Song, K., Du, J., Liu, H., Wen, Z., 2017. Comparison of different satellite bands and vegetation indices for estimation of soil organic matter based on simulated spectral configuration. Agric. For. Meteorol. 244-245, 57–71.
Jones, P.N., Carberry, P.S., 1994. A technique to develop and validate simulation-models. Agric. Syst. 46 (4), 427–442.
Kang, S., Shi, W., Zhang, J., 2000. An improved water-use efficiency for maize grown under regulated deficit irrigation. Field Crops Res. 67 (3), 207–214.
Kang, S., Hao, X., Du, T., Tong, L., Su, X., Lu, H., Li, X., Huo, Z., Li, S., Ding, R., 2017. Improving agricultural water productivity to ensure food security in China under changing environment: from research to practice. Agric. Water Manag. 179, 5–17.
Kang, S., Zhang, J., 2004. Controlled alternate partial root-zone irrigation: its physiological consequences and impact on water use efficiency. J. Exp. Bot. 55 (407), 2437–2446.
Katerji, N., Campi, P., Mastrorilli, M., 2013. Productivity, evapotranspiration, and water use efficiency of corn and tomato crops simulated by AquaCrop under contrasting water stress conditions in the Mediterranean region. Agric. Water Manag. 130, 14–26.
Kemanian, A.R., Stöckle, C.O., Huggins, D.R., Viega, L.M., 2007. A simple method to estimate harvest index in grain crops. Field Crops Res. 103 (3), 208–216.
Li, S., Kang, S., Zhang, L., Ortega-Farias, S., Li, F., Du, T., Tong, L., Wang, S., Ingman, M., Guo, W., 2013. Measuring and modeling maize evapotranspiration under plastic film-mulching condition. J. Hydrol. 503 (1), 153–168.
Mabhaudhi, T., Modi, A.T., Beletse, Y.G., 2014. Parameterisation and evaluation of the FAO-AquaCrop model for a South African taro (Colocasia esculenta L. Schott) landrace. Agric. For. Meteorol. 192-193, 132–139.
Minhas, B.S., Parikh, K.S., Srinivasan, T.N., 1974. Toward the structure of a production function for wheat yields with dated inputs of irrigation water. Water Resour. Res. 10 (3), 383–393.
Muchow, R., 1989. Comparative productivity of maize, sorghum and pearl millet in a semi-arid tropical environment II. Effect of water deficits. Field Crops Res. 20 (3), 207–219.
Pereira, L.S., Paredes, P., Rodrigues, G.C., Neves, M., 2015. Modelingmalt barley water use and evapotranspiration partitioning in two contrasting rainfall years. Assessing AquaCrop and SIMDualKc models. Agric. Water Manag. 159, 239–254.
Perry, C., Steduto, P., Allen, R.G., Burt, C.M., 2009. Increasing productivity in irrigated agriculture: agronomic constraints and hydrological realities. Agric. Water Manag. 96 (11), 1517–1524.
Raes, D., Steduto, P., Hsiao, T.C., Fereres, E., 2009. AquaCrop-the FAO crop model to simulate yield response to water: II. Main algorithms and software description. Agron. J. 101 (3), 438–447.
Raes, D., Steduto, P., Hsiao, T.C., Fereres, E., 2012. Reference Manual, Chapter 3-AquaCrop, Version 4.0. FAO, Land and Water Division, Rome, Italy 300p.
Ran, H., Kang, S., Li, F., Tong, L., Du, T., 2016. Effects of irrigation and nitrogen management on hybrid maize seed production in north-west China. Front. Agric. Sci. Eng. 3 (1), 55–64.
Ran, H., Kang, S., Li, F., Du, T., Ding, R., Li, S., Tong, L., 2017a. Responses of water productivity to irrigation and N supply for hybrid maize seed production in an arid region of Northwest China. J. Arid Land 9 (4), 504–514.
Ran, H., Kang, S., Li, F., Tong, L., Ding, R., Du, T., Li, S., Zhang, X., 2017b. Performance of AquaCrop and SIMDualKc models in evapotranspiration partitioning on full and deficit irrigated maize for seed production under plastic film-mulch in an arid region of China. Agric. Syst. 151, 20–32.
Ran, H., Kang, S., Li, F., Du, T., Tong, L., Li, S., Ding, R., 2018. Parameterization of the AquaCrop model for full and deficit irrigated maize for seed production in arid Northwest China. Agric. Water Manag. 203, 438–450.
Razzaghi, F., Zhou, Z., Andersen, M.N., Plauborg, F., 2017. Simulation of potato yield in temperate condition by the AquaCrop model. Agric. Water Manag. 191, 113–123.
Richards, R., Townley-Smith, T., 1987. Variation in leaf area development and its effect on water use, yield and harvest index of droughted wheat. Crop Pasture Sci. 38 (6), 983–992.
Sadras, V., Connor, D., 1991. Physiological basis of the response of harvest index to the fraction of water transpired after anthesis: a simple model to estimate harvest index for determinate species. Field Crops Res. 26 (3), 227–239.
Santhi, C., Arnold, J.G., Williams, J.R., Dugas, W.A., Srinivasan, R., Hauck, L.M., 2001. Validation of the SWAT model on a large river basin with point and nonpoint sources. J. Am. Water Resour. Assoc. 37 (5), 1169–1188.
Steduto, P., 2003. Biomass water-productivity. Comparing the Growth-Engines of Crop Models. FAO Expert Consultation on Crop Water Productivity under Deficient Water Supply. pp. 26–28.
Steduto, P., Albrizio, R., 2005. Resource use efficiency of field-grown sunflower, sorghum, wheat and chickpea: II. Water use efficiency and comparison with radiation use efficiency. Agric. For. Meteorol. 130, 269–281.
Steduto, P., Hsiao, T., Fereres, E., 2007. On the conservative behavior of biomass water productivity. Irrig. Sci. 25, 189–207.
Steduto, P., Hsiao, T.C., Raes, D., Fereres, E., 2009. AquaCrop—the FAO crop model to simulate yield response to water: I. Concepts and underlying principles. Agron. J. 101 (3), 426–437.
Steduto, P., Hsiao, T.C., Fereres, E., Raes, D., 2012. Crop Yield Response to Water. FAO Irrigation and Drainage Paper 66. FAO, Rome, Italy 500p.
Stella, P., Lamaud, E., Brunet, Y., Bonnefond, J.M., Loustau, D., Irvine, M., 2009. Simultaneous measurements of CO2 and water exchanges over three agroecosystems in South-West France. Biogeosciences 6 (12), 2957–2971.
Stewart, J.I., Hagan, R.M., Pruitt, W.O., Danielson, R.E., Franklin, W.T., Hanks, R.J., Riley, J.P., Jackson, E.B., 1977. Optimizing Crop Production through Control of Water and Salinity Levels in the Soil. Reports. Paper 67.
Tavakoli, A.R., Mahdavi Moghadam, M., Sepaskhah, A.R., 2015. Evaluation of the AquaCrop model for barley production under deficit irrigation and rainfed condition in Iran. Agric. Water Manag. 161, 136–146.
Thornley, J.H.M., 1976. Mathematical Models in Plant Physiology. Academic Press, New York 318p.
Thorp, K.R., Batchelor, W.D., Paz, J.O., Kaleita, A.L., Dejonge, K.C., 2007. Using cross validation to evaluate Ceres-Maize yield simulations within a decision support system for precision agriculture. Trans. Asabe 50 (4), 1467–1479.
Toumi, J., Er-Raki, S., Ezzahar, J., Khabba, S., Jarlan, L., Chehbouni, A., 2016. Performance assessment of AquaCrop model for estimating evapotranspiration, soil water content and grain yield of winter wheat in Tensift Al Haouz (Morocco): application to irrigation management. Agric. Water Manag. 163, 219–235.
Wang, H., Liu, C., 2003. Experimental study on crop photosynthesis, transpiration and high efficient water use. Yingyong Shengtai Xuebao 14 (10), 1632–1636.
Wang, X., Wang, Q., Fan, J., Fu, Q., 2013. Evaluation of the AquaCrop model for simulating the impact of water deficits and different irrigation regimes on the biomass and yield of winter wheat grown on China's Loess Plateau. Agric. Water Manag. 129, 95–104.
Zhan, L., Yang, H., Lei, H., 2016. Analysis of corn water consumption, carbon assimilation and ecosystem water use efficiency based on flux observations. Trans. Chin. Soc. Agric. Eng. 32 (Supp.1), 88–93 in Chinese with English abstract.
Zhao, F., Yu, G., Li, S., Ren, C., Sun, X., Mi, N., Li, J., Ouyang, Z., 2007. Canopy water use efficiency of winter wheat in the North China Plain. Agric. Water Manag. 93 (3), 99–108.